Chapters 3 & 4

Advanced Measurements in Semiconductor Lasers

Ultra-Short Pulse Generation

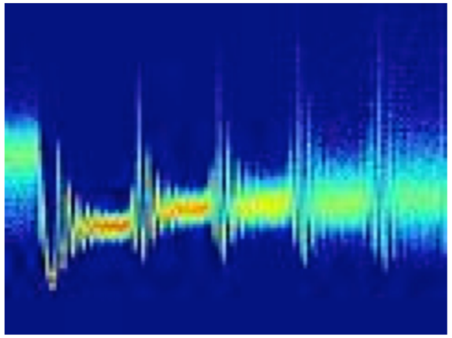

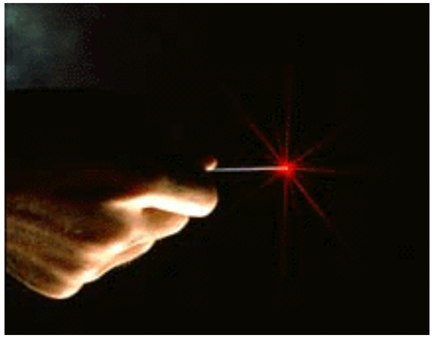

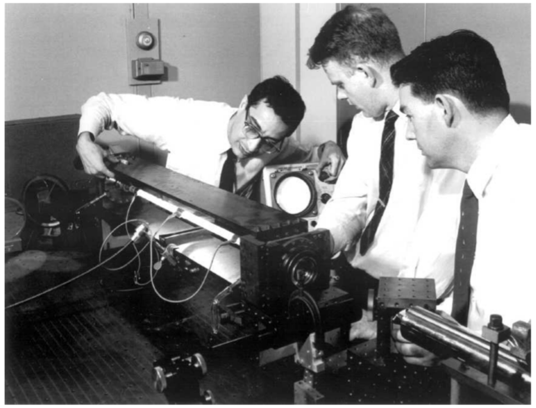

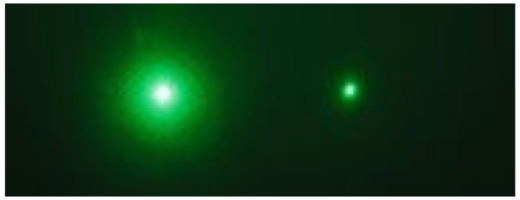

Introduction

- The fast growing use of semiconductor lasers in various fields including fiber telecommunication systems, optical data storage, remote sensing places **very stringent requirements on device performance**
- A **detailed understanding of physical processes** governing the behavior of laser diodes is required
- **Electrical and optical techniques** give complimentary information on the operation of the laser diodes
- Physical processes **below threshold** are critical in determining the operating point of the laser (device performance)
- Leakage current or wavelength chirp can be deduced from **above threshold measurements**
- These measurements provide critical **experimental feedback in the process of laser diode optimization.**

Laser Structure

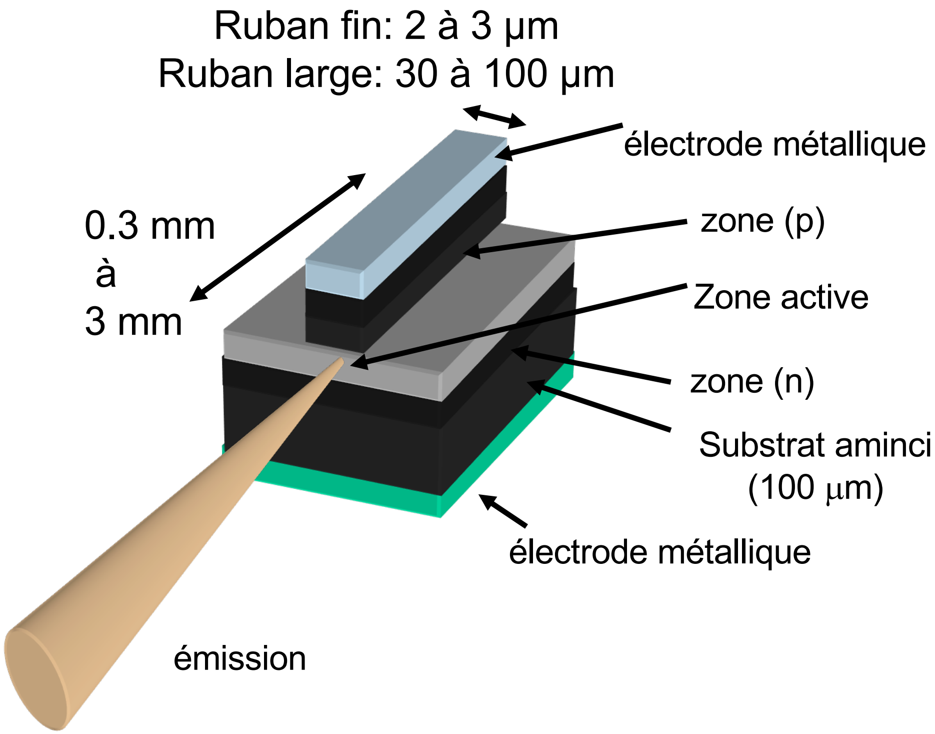
Ruban fin: 2 à 3 µm
Ruban large: 30 à 100 µm

0.3 mm
à
3 mm

électrode métallique

zone (p)

Zone active

zone (n)

Substrat aminci
(100 μm)

électrode métallique

émission

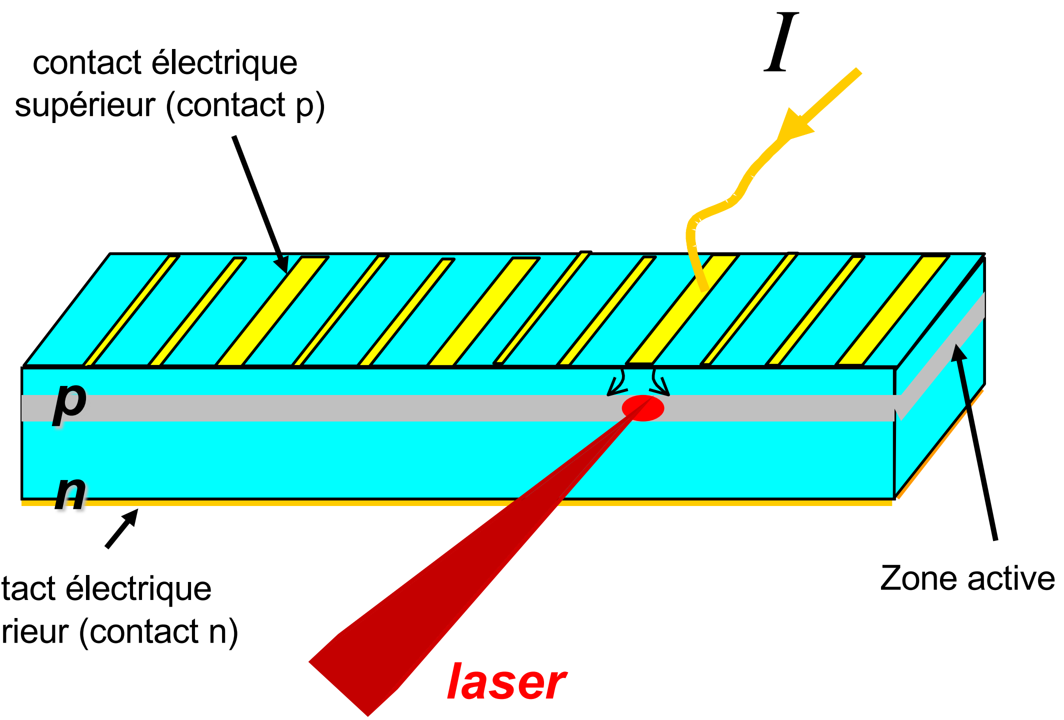
contact électrique
supérieur (contact p)

I

p

n

contact électrique
inférieur (contact n)

Zone active

laser

Laser Structure

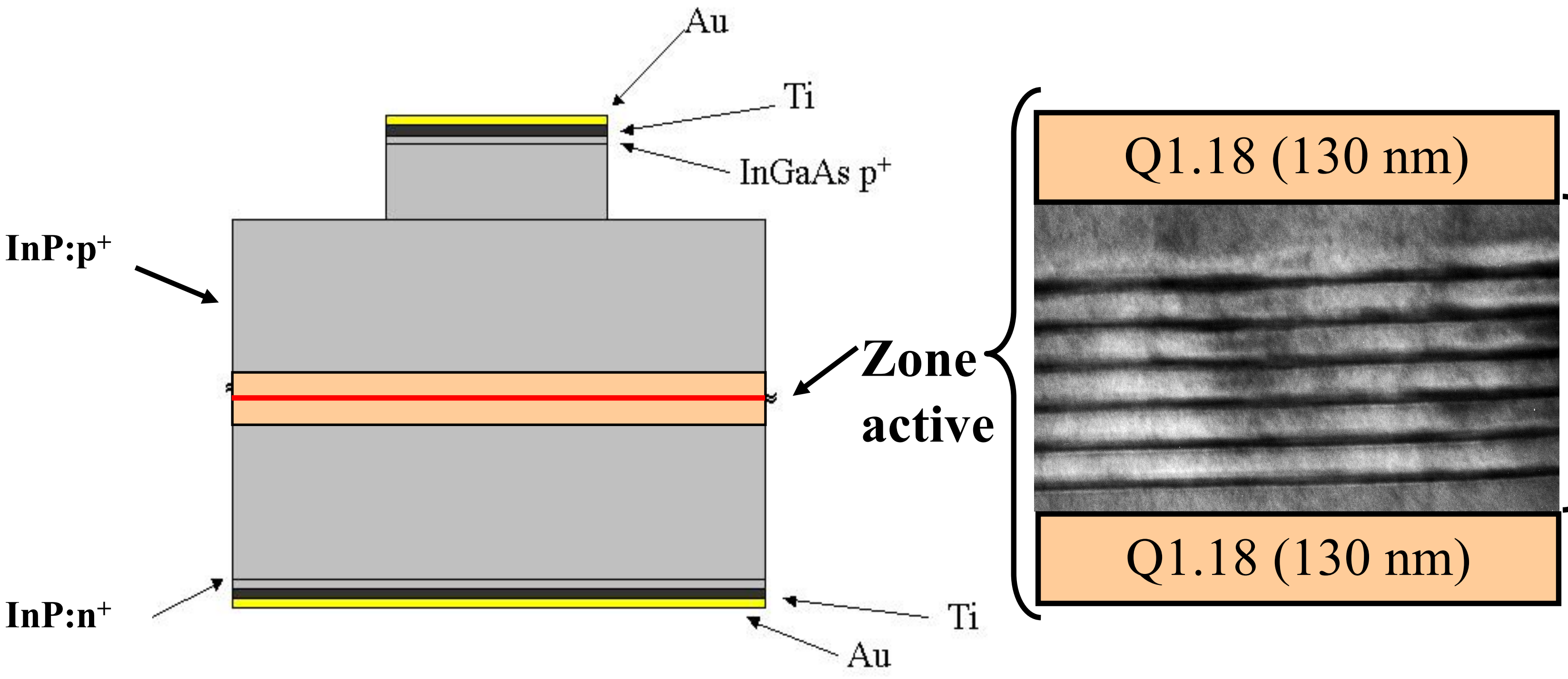

Milieu émetteur:
-Puits quantiques
-îlots quantiques

Laser Testing

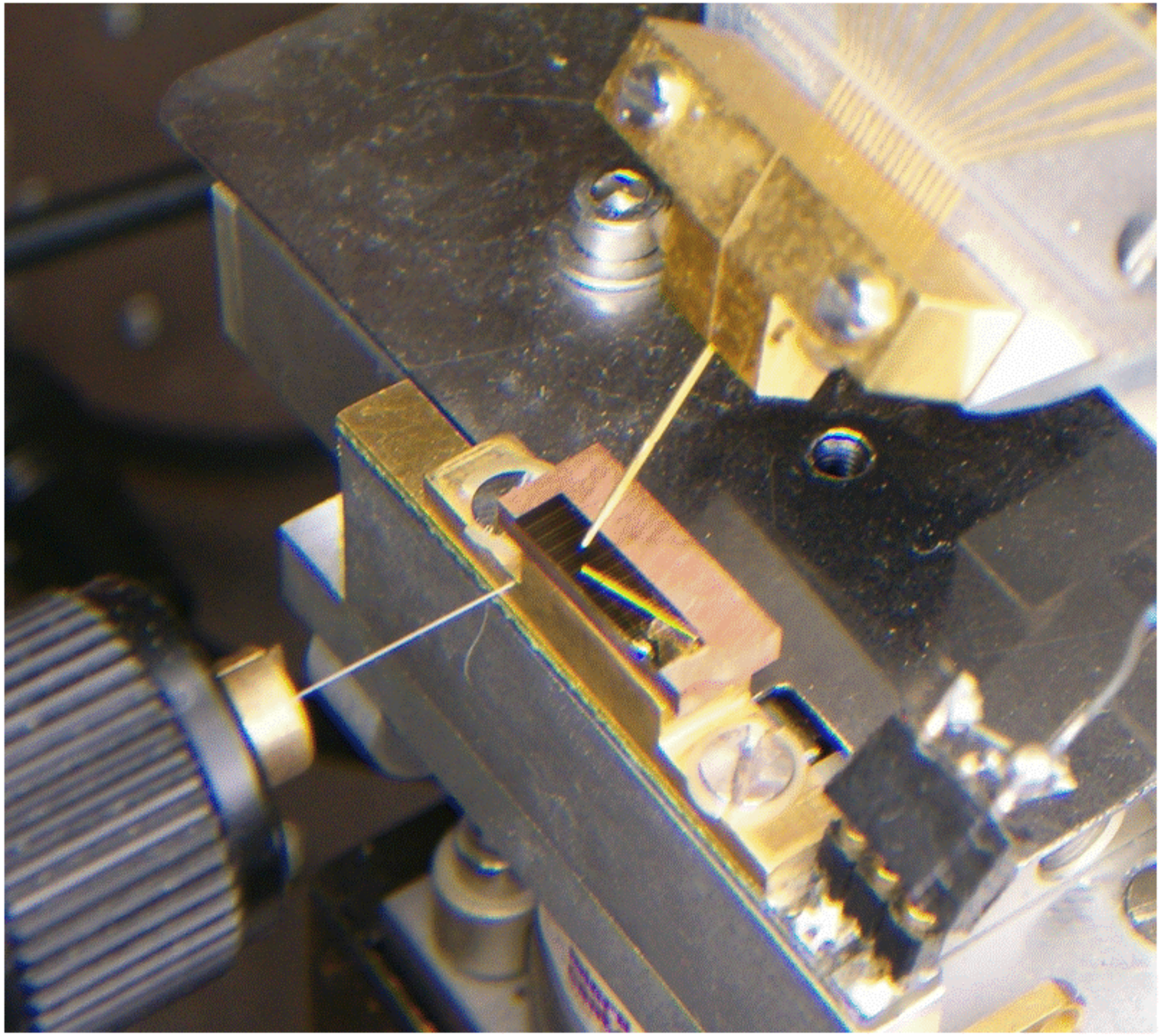

Laser Testing

❑ Static measurements

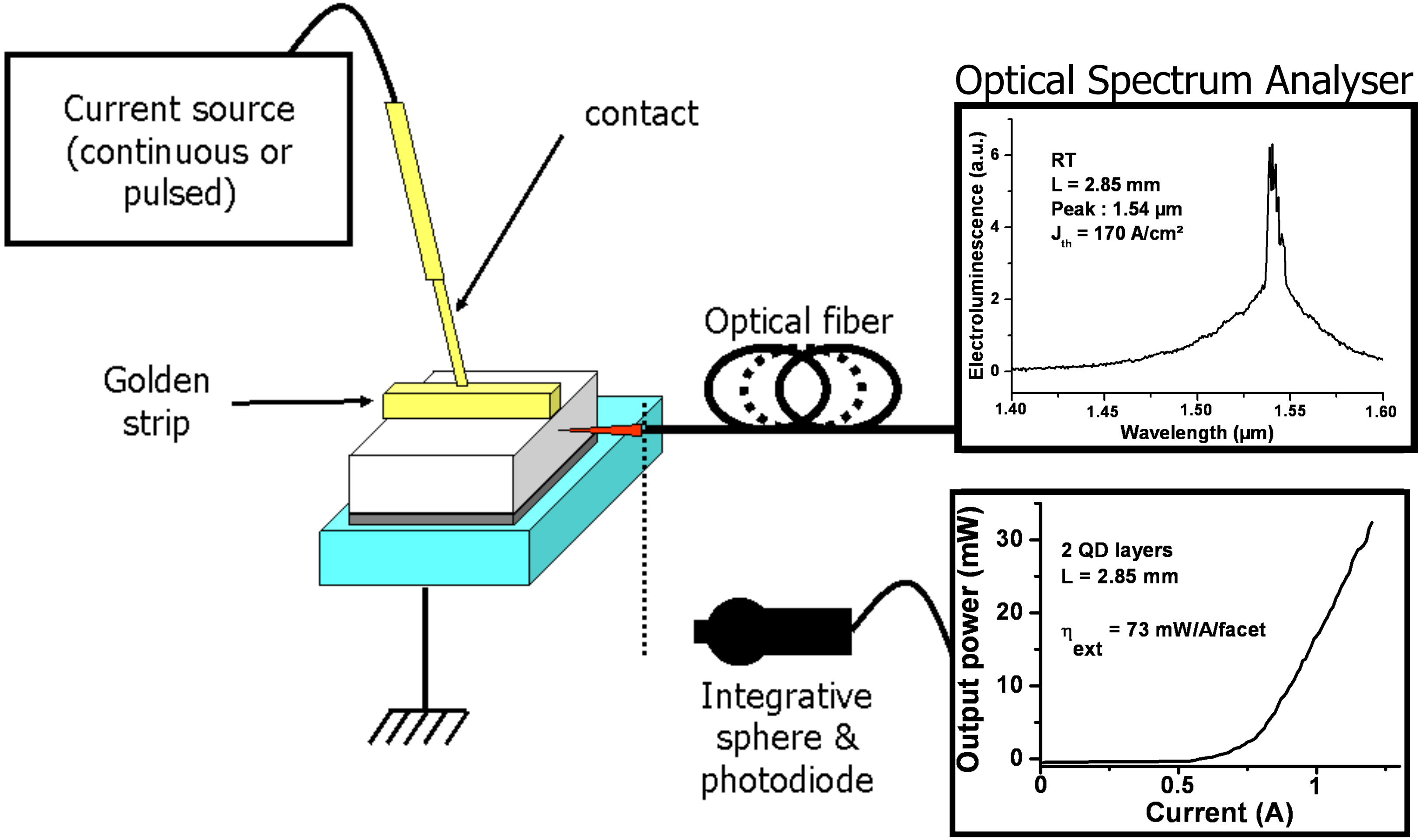

I-V Characteristics

- I(V) allows to estimate the **quality of the junction**

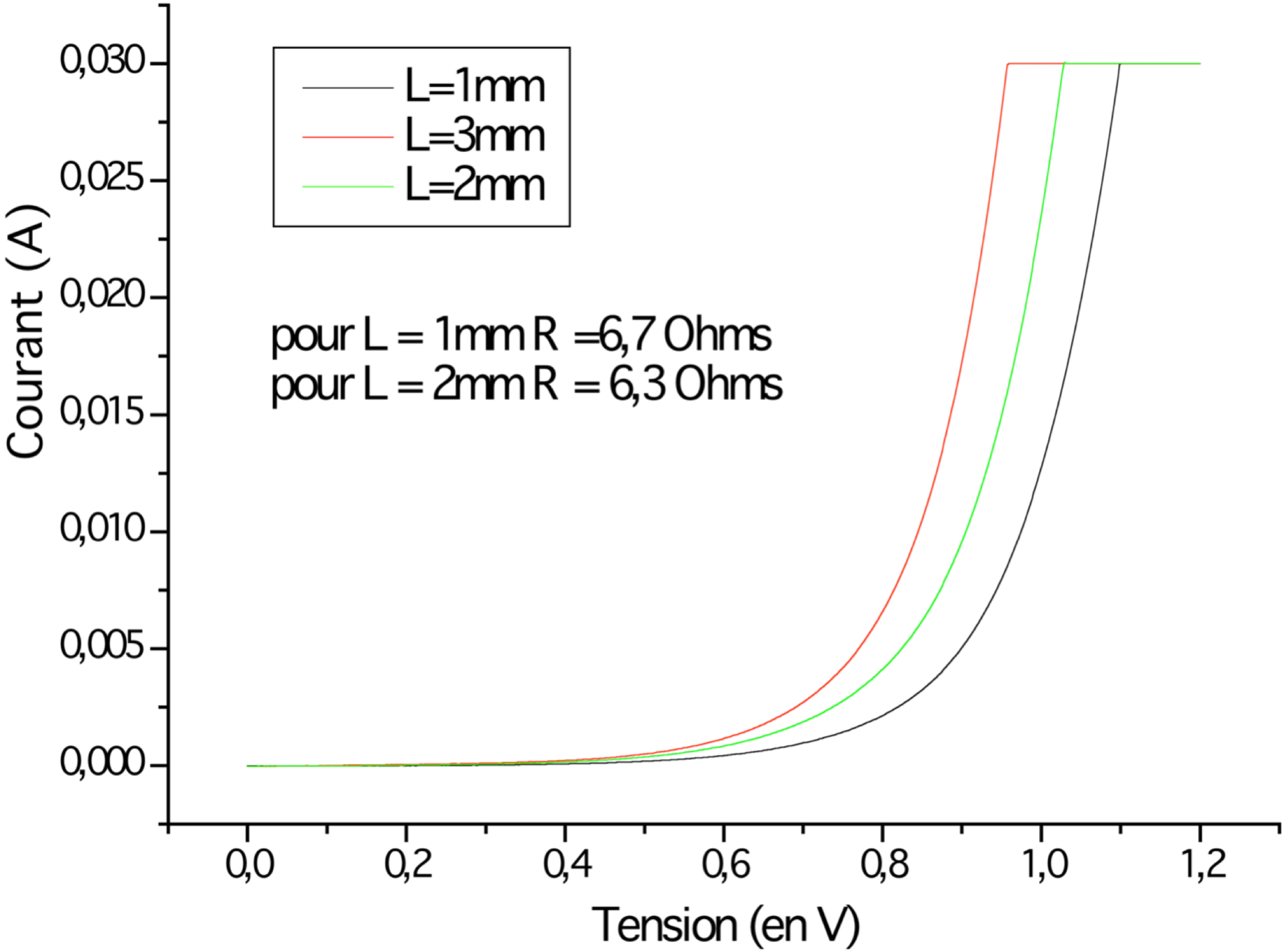

First-Step Exp.

- ☐ LCC gives I_{th}, external efficiency
- ☐ I_{th} versus T gives the **temperature characteristics** T_0
- ☐ J_{th} versus 1/L gives the **transparency current density**

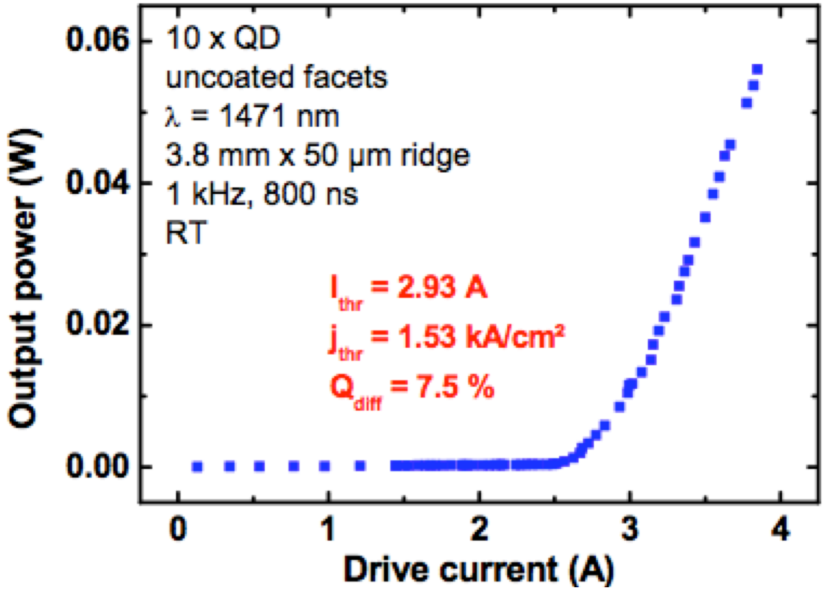

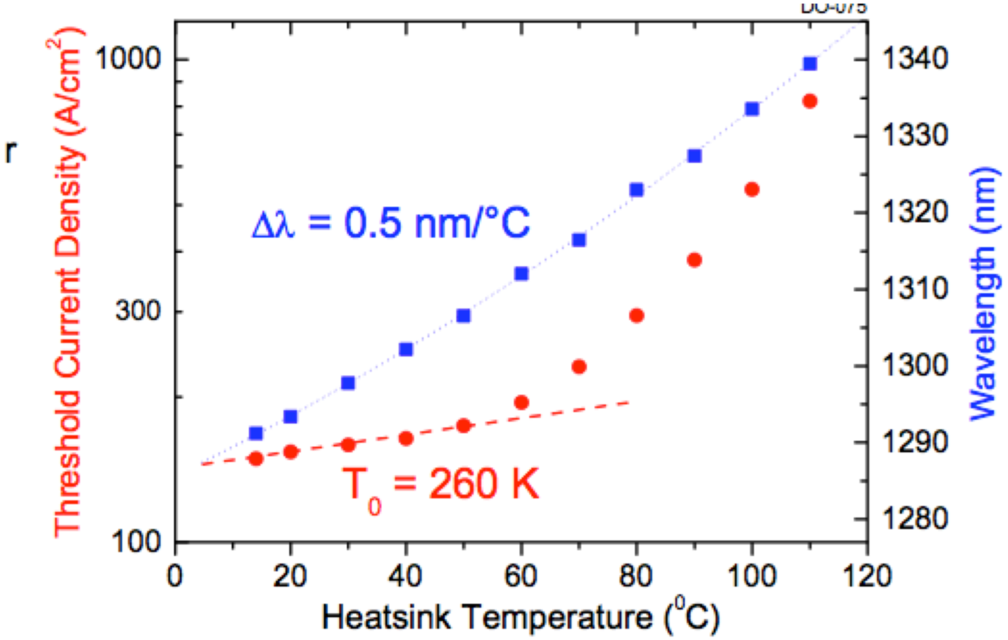

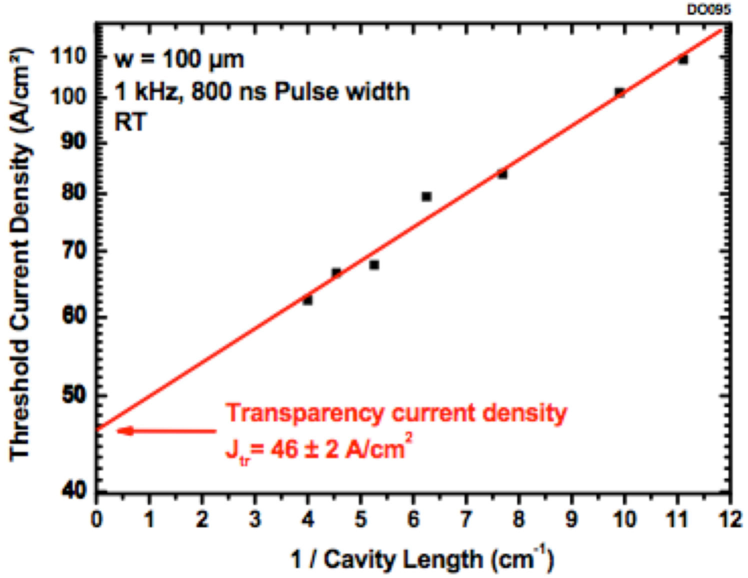

ASE Spectrum

❑ Optical gain influences the operating conditions not only the basic **output characteristics**, such as the threshold current, but also the temperature dependence as well as **high-speed performance of the laser**

❑ Figure to the right shows spectra of **amplified spontaneous emission (ASE)** for an 1.3µm buried heterostructure semiconductor laser

❑ B. Hakki and T. Paoli proposed to determine the modal optical gain from the **contrast of the ASE spectra where r(λ) is the peak-to-valley ratio**

$$g(\lambda) = \frac{1}{L}\ln\left(\frac{\sqrt{r(\lambda)}-1}{\sqrt{r(\lambda)}+1}\right) \quad r(\lambda) = \frac{I_{max}(\lambda)}{I_{min}(\lambda)}$$

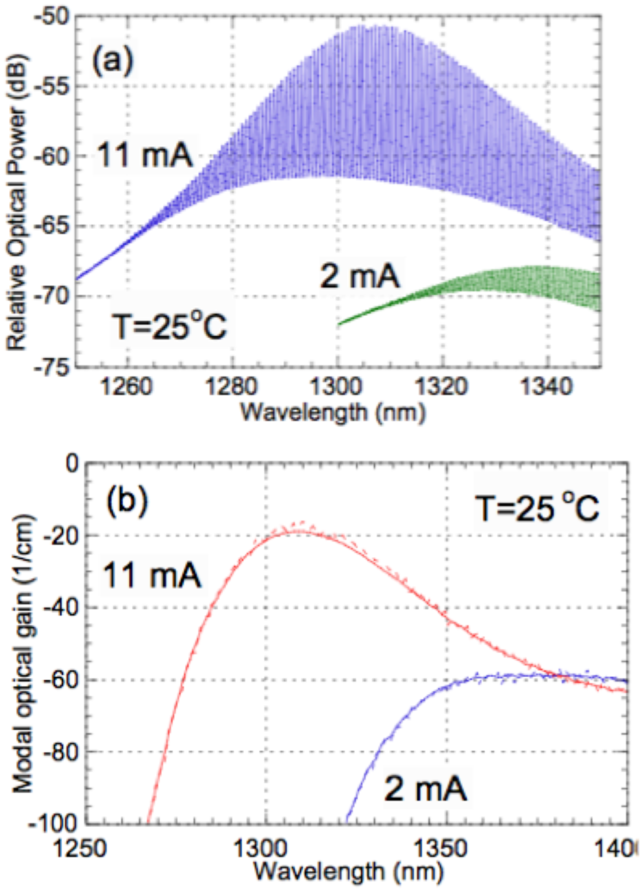

TSE Spectrum

- **True Spontaneous Emission** (TSE) spectra is recorded **from the side of an uncoated laser** at different currents

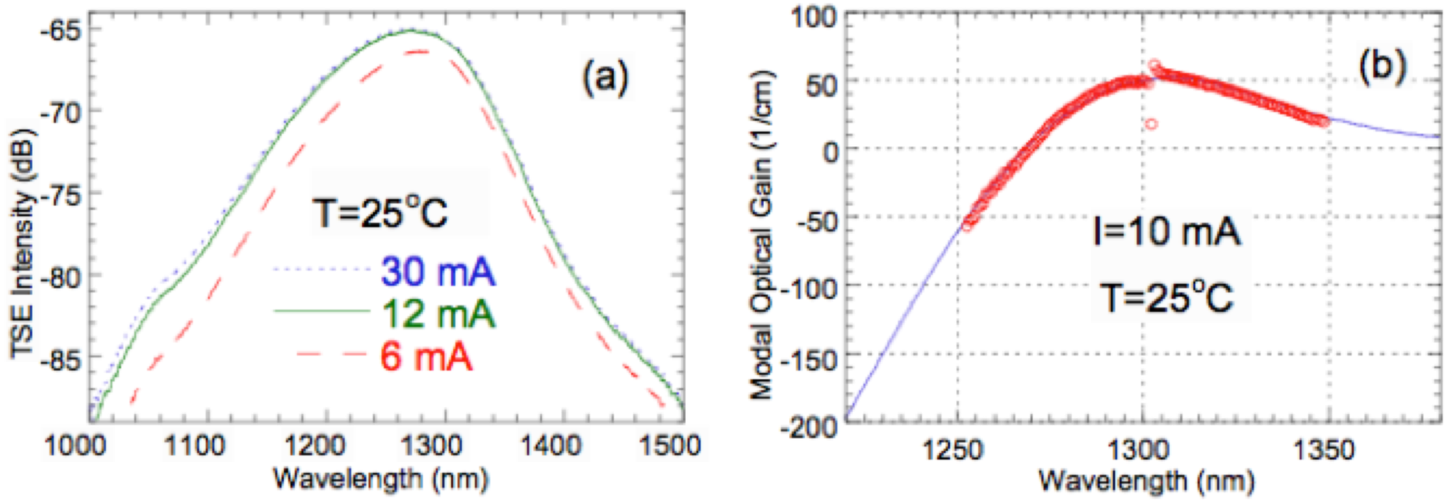

- TSE spectrum is broader with no FP ripples and extends much further into high energies than the ASE because the **TSE is not affected by re-absorption in the active layer**

- TSE spectrum is not affected by the value or the spectral dependence of the mirror loss or grating ⇒ **true information about the optical gain in case ASE technique is not suitable**

TSE / QD Lasers

❑ Results on GaAs:

- Expertise on recombination mechanisms with both theory & experimental set-ups
- Importance of **non-radiative recombination processes**
- Predominance of **Auger effect in long wavelength laser**

Marko et al. IEEE J. Sel. Top. Quantum Elec. **9** 1300 (2003)

❑ Experimental set-up

Radiative current linearly linked to integrated spontaneous radiative emission

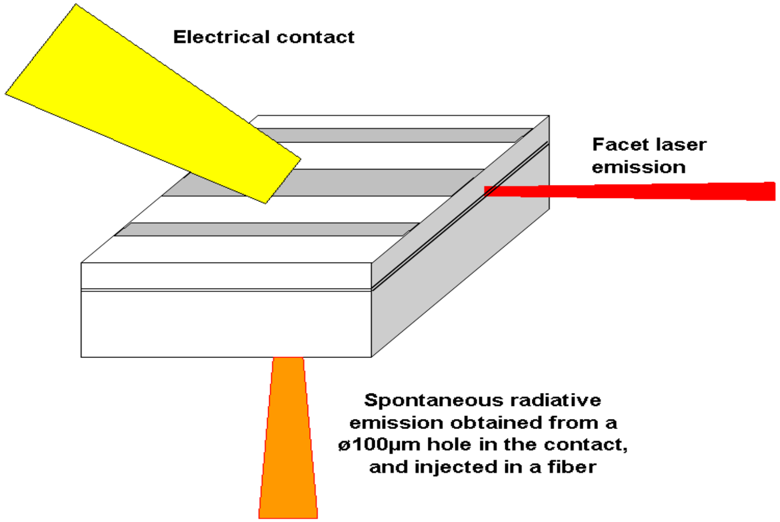

TSE/QD Lasers

- ☐ **Total current:** $j = j_{stim} + j_{rad} + j_{non\_rad}$
- ☐ **At threshold:** $j_{stim} = 0$ ⇨ $j_{th} = j_{rad} + j_{non\_rad}$

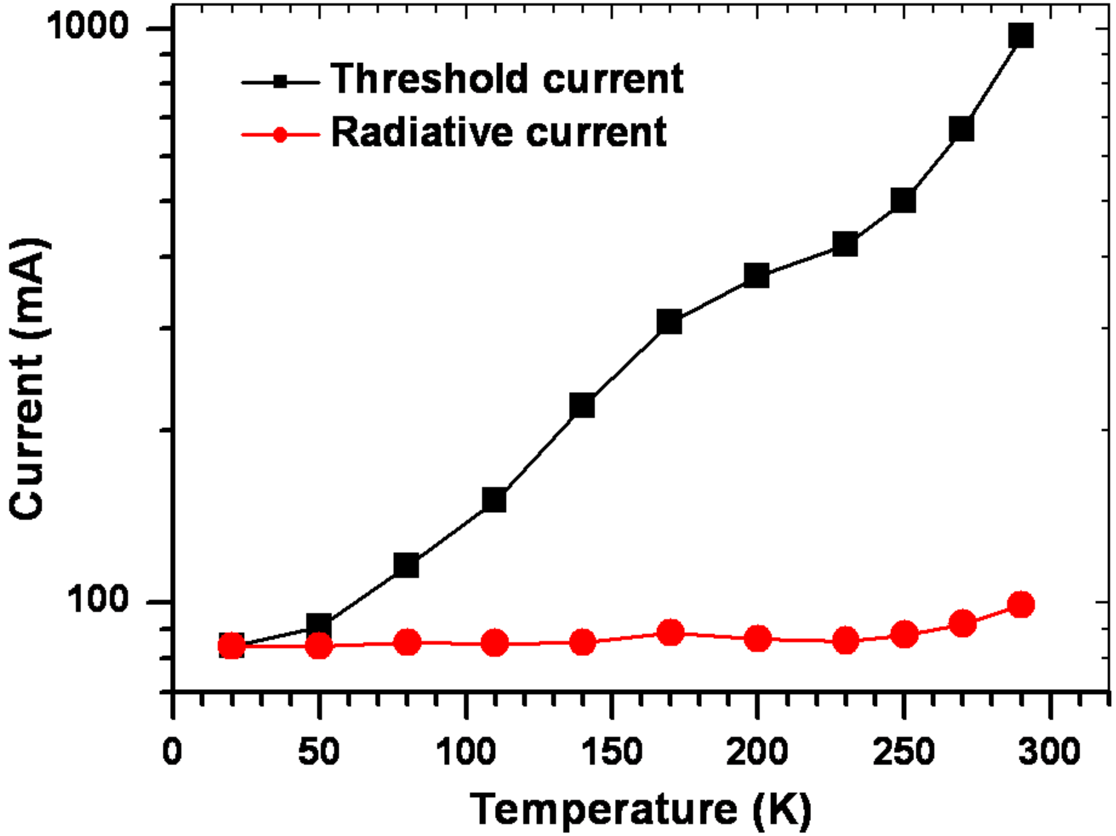

⇨ **Great importance of non radiative recombination**

Pressure Evaluation

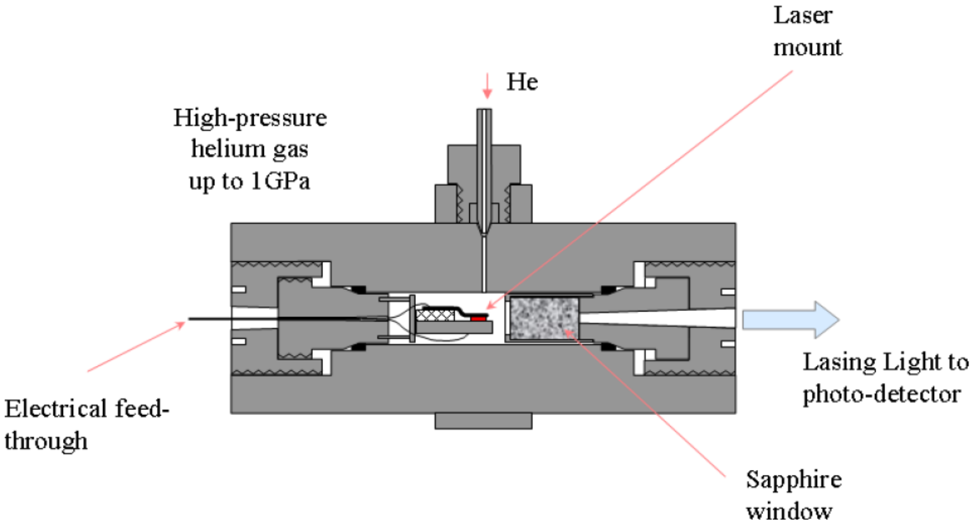

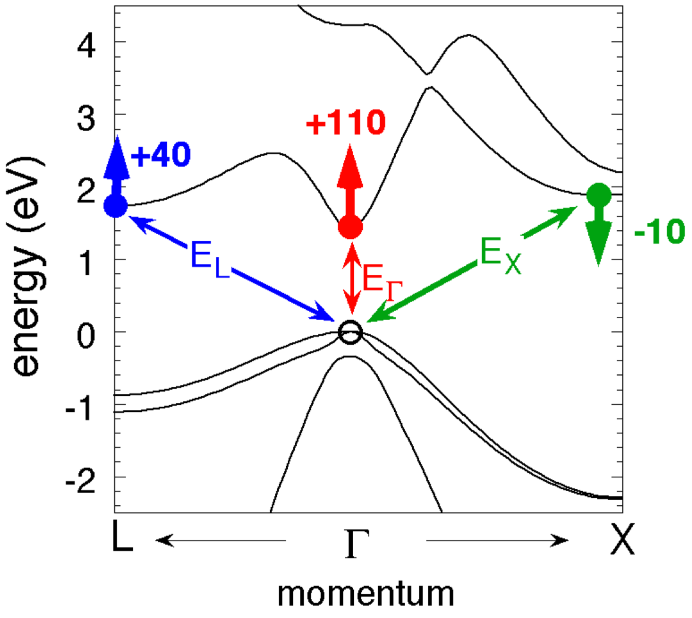

(Marko et al. IEEE J. Sel. Top. Quantum Elec. **9** 1300 (2003))

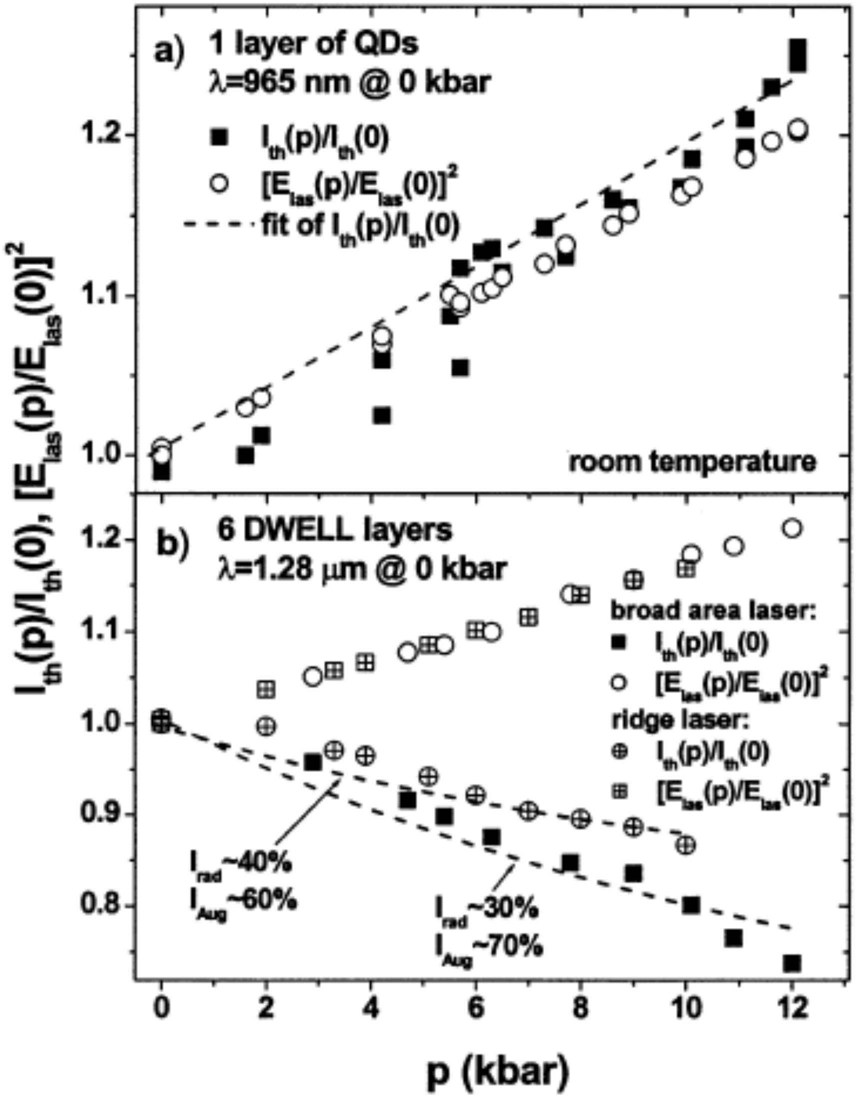

Pressure /QD Lasers

- Nature of these **non-radiative recombination** ?

$$j_{non\_rad} = j_{leak} + j_{auger}$$

When P ↗ : j_{rad} ↗ j_{leak} ↗ while j_{auger} ↘

(Marko et al. IEEE J. Sel. Top. Quantum Elec. **9** 1300 (2003))

- Measurement of **j_{th} as a function of the pressure**

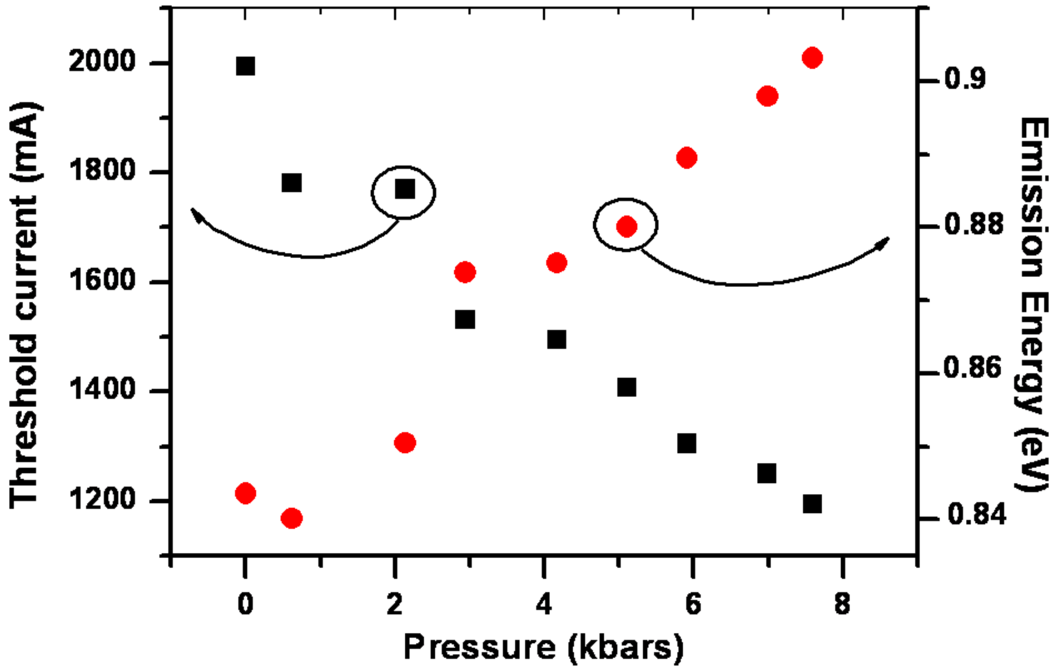

j_{th} ↘ : signature of the predominance of **Auger effect**

Optical Loss

- ❑ Optical loss are related to the **free-carrier absorption (intraband process) and scattering loss on the waveguide nonuniformities**

- ❑ Using a **set of lasers, varying in length** allow to estimate the average value of loss as well as the internal quantum efficiency

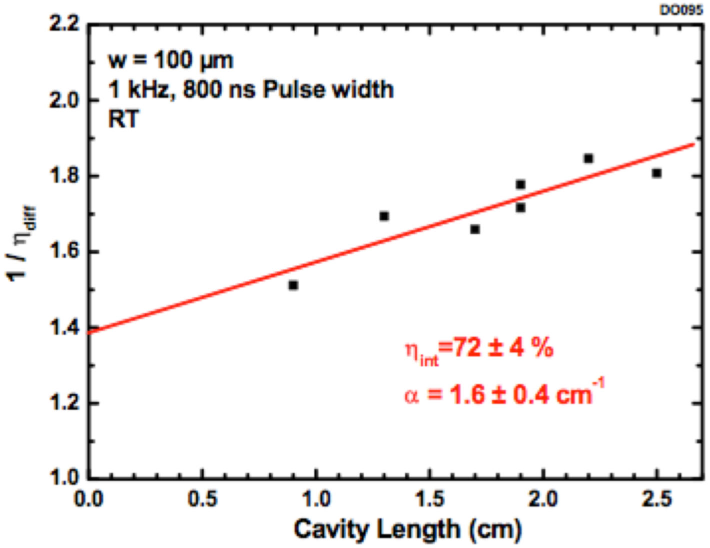

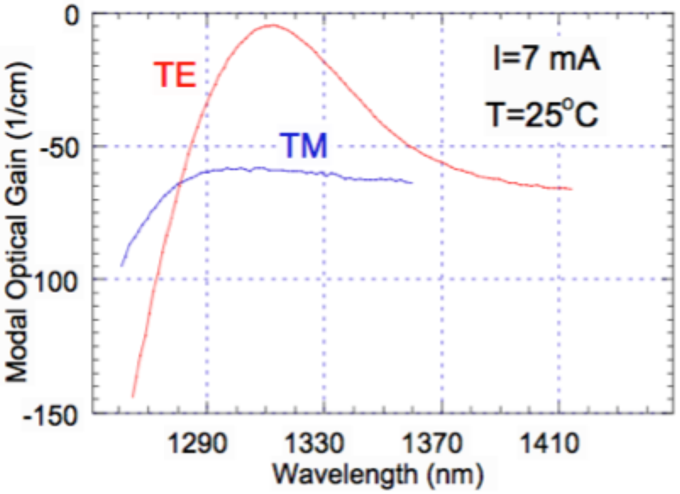

- ❑ **Intersection of the gain curves in TE and TM polarizations** (optical gain does not depend on the polarization when the material gain is zero)

- ❑ **Modal optical gain equals total loss if the material optical gain is zero** (at the transition point between absorption and gain)

Carrier Leakage

- Collection of the light resulting from **recombination of carriers outside the active region**

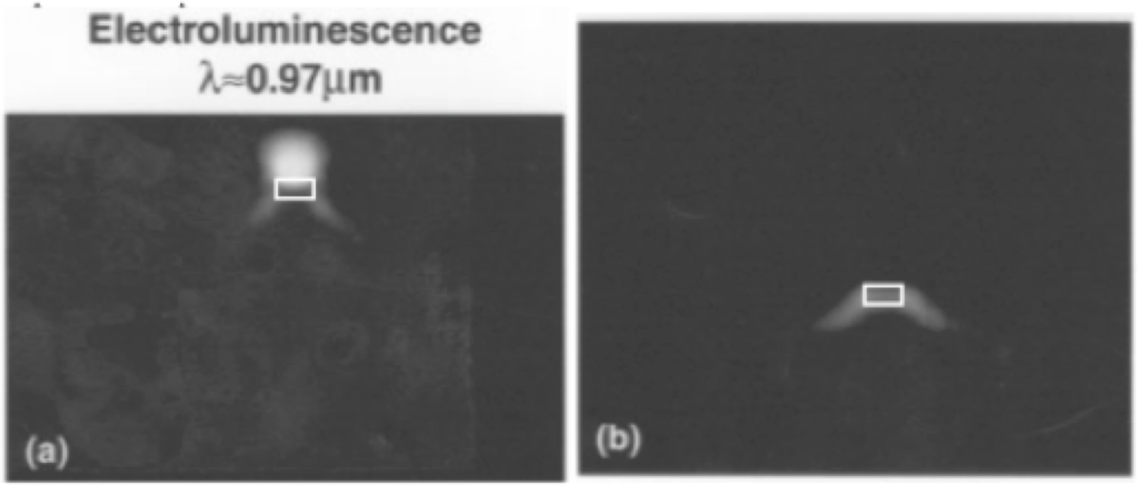

- Significant electron leakage can occur in double heterostructures constituting one of the mechanisms of **sub-linearity of the LCC and also of the temperature dependence of the threshold current in laser diodes**

- Laser structures with **low carrier overflow into barriers and SCH** (separate confinement area) layer exhibit **better high-temperature performance**

RIN

- Relative intensity noise (RIN) is associated with the **fluctuation of the concentrations in photon and electron systems caused by spontaneous emission light events**

- Deviation of the electron and photon densities from equilibrium values lead to their **damped oscillations with the frequency of electron-photon resonance and damping factor**

$$RIN = \frac{4}{\pi}\delta f \frac{f^2 + (\gamma^*/2\pi)}{(f_R^2 - f^2)^2 + f^2(\gamma/2\pi)^2}$$

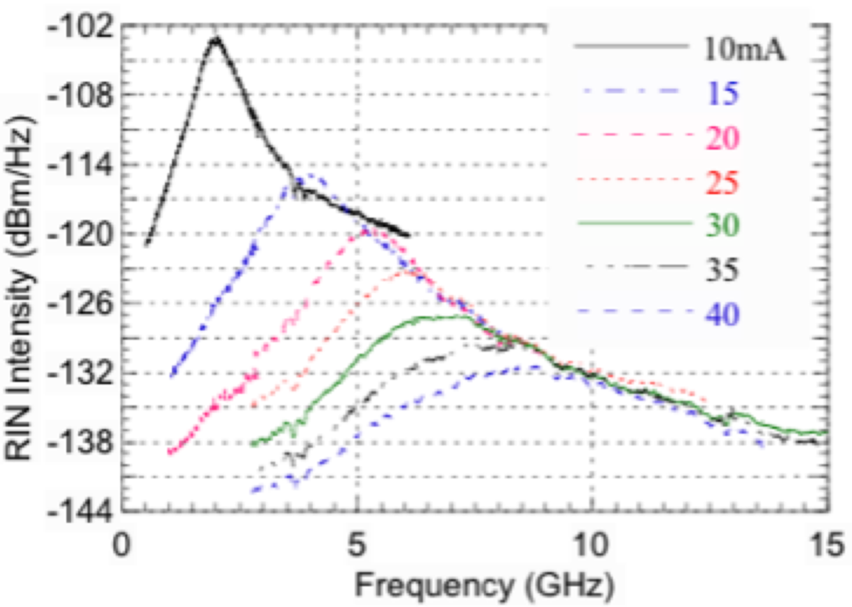

- Figure to the left shows the RIN spectra for a 1.3 µm InGaAsP/InP MQW laser at the different bias condition

- **Resonance frequency, damping factor and linewidth can be determined from curve-fitting**

Modulation Response

- Laser's optical modulation response at different DC biases, measured using a **network analyzer with a high-speed pin detector**

- Additional drooping of the response curves has been attributed to **carrier transport through the SCH layers and the carrier capture and thermoionic emission processes in QW lasers**

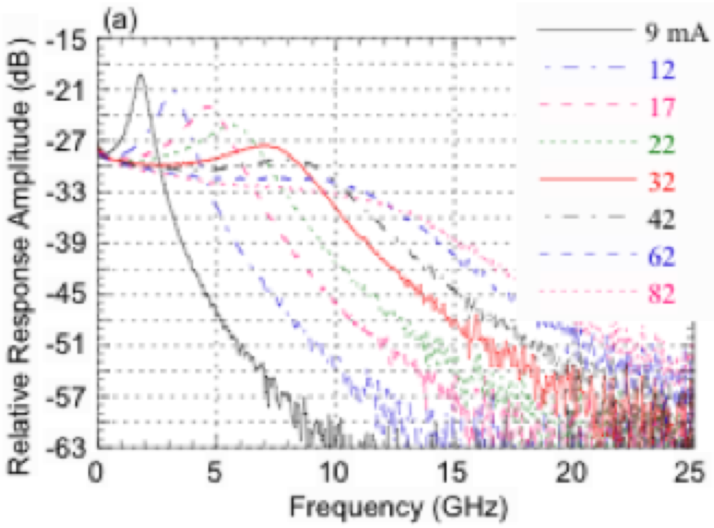

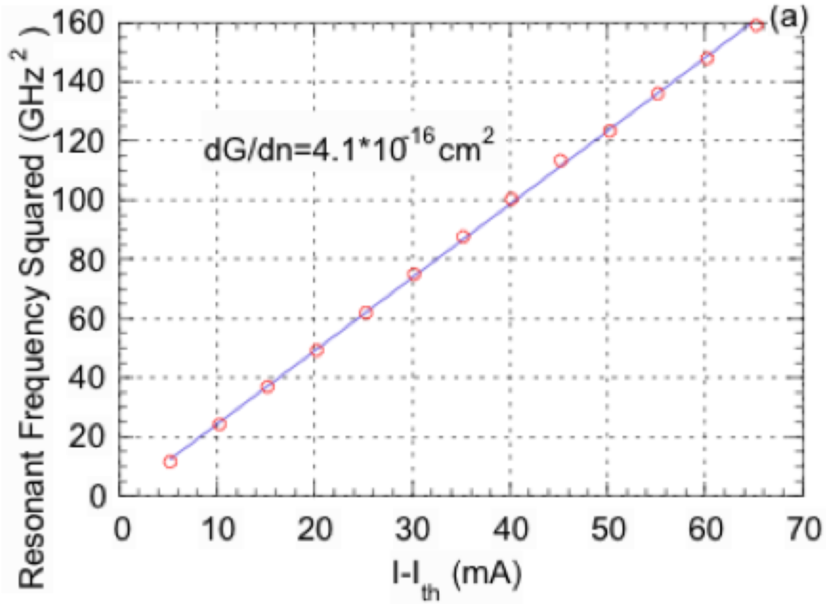

$$\omega_R \approx \sqrt{\frac{\frac{c}{n_{eff}}\frac{dG}{dN}S_0}{\tau_p(1+\epsilon_S S_0)}} \qquad \gamma = K f_R^2 + \gamma_0 \qquad H(\omega) = \frac{\omega_R^2}{\omega_R^2 - \omega^2 + j\omega\gamma}$$

Carrier Lifetime

- ☐ The simplest equivalent circuit of a semiconductor laser **below threshold can be derived from the rate equation (Small-Signals)**

- ☐ Active layer represented as a **RC circuit with characteristic time equal to the differential carrier lifetime**

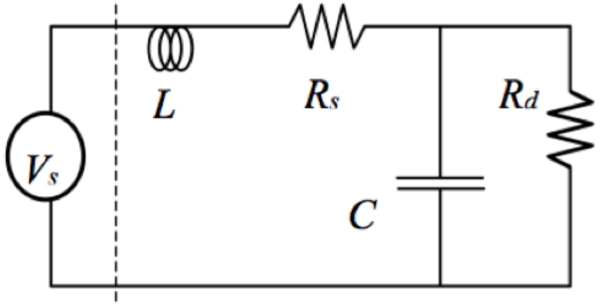

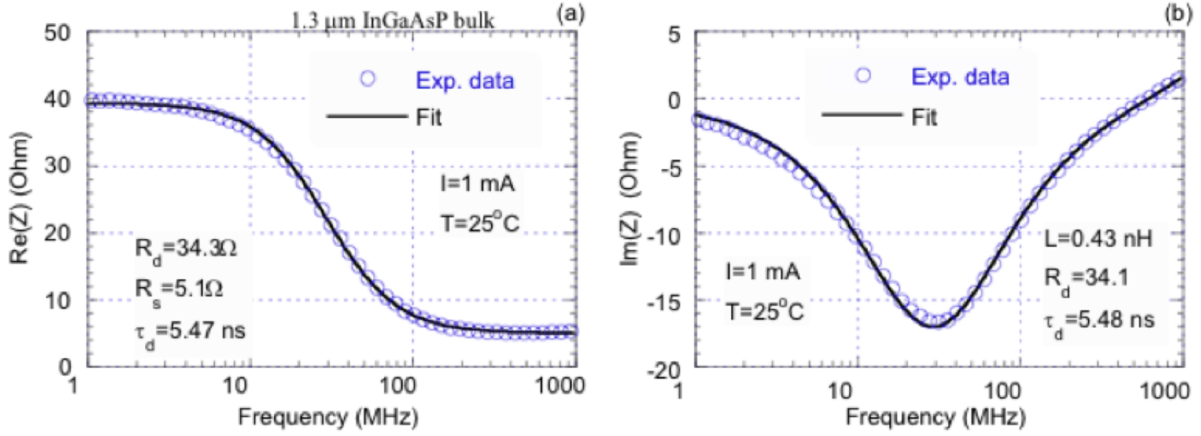

$$Z(j\omega) = j\omega L + R_s + \frac{R_d}{1 + j\omega\tau_d}$$

$$\tau_d = R_d C$$

- ☐ Laser impedance below threshold is **frequency-dependent**
  ⇒ **the differential carrier lifetime can be extracted**

Carrier Lifetime

- ❑ This technique is for determining the differential carrier lifetime via a **small-signal current step excitation**

- ❑ This technique has the **disadvantage of high noise if the excitation signal is small**

- ❑ The measured optical response curve is shown to the right (circles) and was corrected (squares) and then fit to a single pole roll-off form **from which the differential carrier lifetime can be extracted**

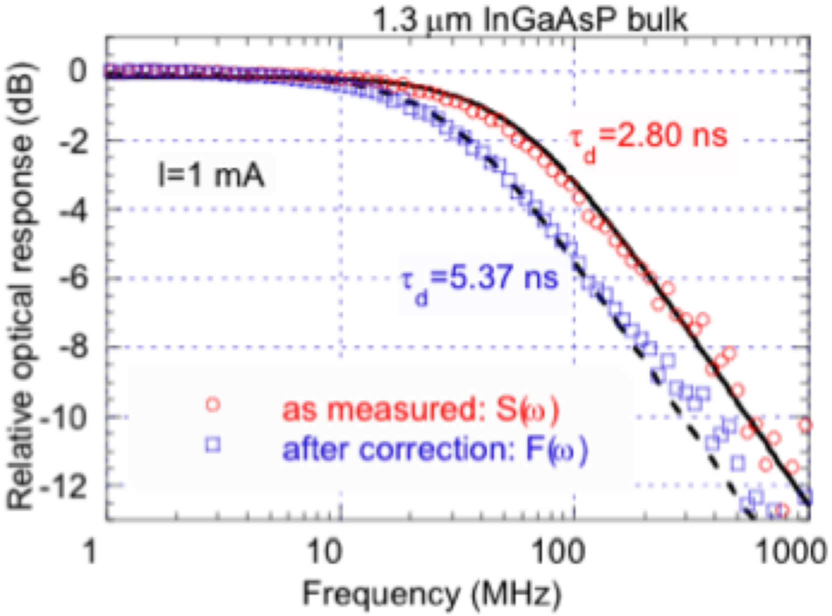

$$d\delta N(\omega) = \frac{1}{eV_{act}} \frac{\delta V}{r + Z(j\omega)} \frac{\tau_d}{1 + j\omega\tau_d}$$

$$F(\omega) = |\delta S(\omega)||r + Z(\omega)| \propto \frac{1}{\sqrt{1 + (\omega\tau_d)^2}}$$

LEF/ASE

❑ By recording the **ASE at different currents below threshold** and measuring the change of the gain and the **wavelength shift of FP peaks** with current ⇒ **LEF and its dependence on the wavelength and current can be determined**

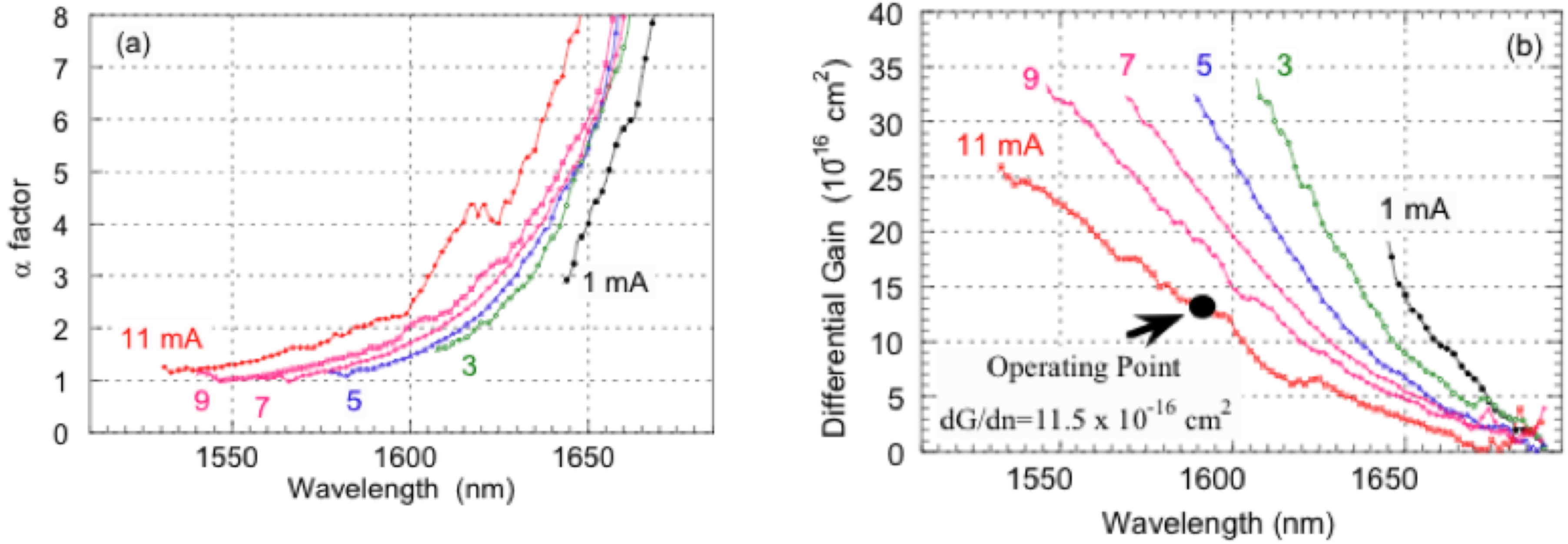

$$\alpha_{HT} = -\frac{4\pi n_{eff}}{\lambda^2}\left(\frac{\partial \lambda}{\partial g}\right)_T$$

LEF/TSE

❑ An alternative measurement technique for LEF determination utilizes the **optical gain spectra determined from TSE**

❑ The gain spectra should be obtained in a **very broad energy range**

❑ Hakki-Paoli technique for extraction of the gain spectra from **amplified spontaneous emission (ASE) from the laser facet does not allow for that**

❑ The ASE measurements are usually easier to perform and more accurate, but sometimes the **TSE type of the measurements are the only available solution**

❑ Both methods described are based on the **below threshold**
⇒ **measurements can give only asymptotic value of the parameters close to threshold**

$$\delta n' = \frac{2}{\pi} P \int_0^{+\infty} \delta n" \frac{\epsilon'}{\epsilon'^2 - \epsilon"^2} d\epsilon' \quad \Longrightarrow \quad \alpha_T(\epsilon) = \frac{\left(\frac{\partial n'}{\partial \mu}\right)_T}{\left(\frac{\partial n"}{\partial \mu}\right)_T} = \frac{2}{\pi} \frac{\epsilon P \int_0^{+\infty} \delta G(\epsilon') \frac{d\epsilon'}{\epsilon'^2 - \epsilon"^2}}{\delta G(\epsilon)_T}$$

Carrier Heating

- ☐ High injection: **significant difference between the lattice temperature and the temperature of the electron-hole-plasma in the active region**
- ☐ Sources of carrier heating above threshold are **injection of energetic carriers from heterobarriers into active layer and free-carrier absorption**
- ☐The first effect depends on the **injection current and the second on the optical field**
- ☐ Since the modal optical gain, wavelength chirp and carrier leakage over the heterobarrier are sensitive to the carrier temperature, **the study of carrier heating is important for improving device design**
- ☐ An interesting experimental technique allows **to measure the rate of change of the carrier plasma temperature with pumping current above threshold**

Carrier Heating

- **Rate of carrier heating:**

$$\frac{dT}{dI} = \frac{4\pi n_{eff}}{(\alpha_{HT} - \alpha_{H\mu})c} \frac{\beta}{\left(\frac{\partial g}{\partial T}\right)_{\mu}}$$

- Coefficient $\beta = dv/dI$ is the chirp parameter

- Equation above establishes the relation **between the rate of carrier heating above threshold and wavelength chirp**

- Coefficients dg/dT_{eh}, α_{HT} and $\alpha_{H\mu}$ **can be determined from the gain measurements**

⇒ dg/dT_{eh}=-0.45=/-0.05 $cm^{-1}K^{-1}$, α_{HT}=2.1+/-0.2 and $\alpha_{H\mu}$=-1.4+/-0.3 and β =156 MHz/mA

- Using these values, the rate of change of **the carrier temperature with current was estimated to be approximately 0.13K/mA**

⇒ The accuracy of the estimation is about 25%

Why Mode-Locking?

- ☐ Digital Communications
- ☐ Extremely **Short Duration Pulses**
  - Picosecond (10^{-12} s)
  - Femtosecond (10^{-15} s)
- ☐ Optical Transmission Speeds
  - **Speed of light** ~ 3×10^{8} m/s

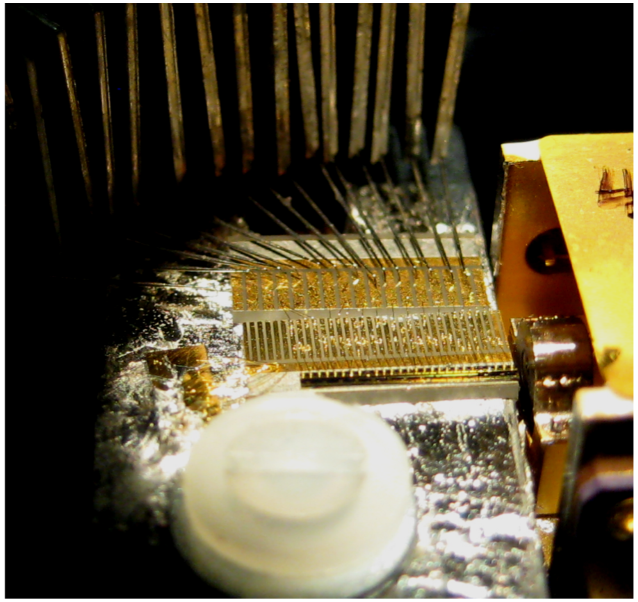

Mode-Locked Laser

Mode Locking

- T_R is the cavity round trip time
  $1/T_R$ is the repetition rate

$$T_R = \frac{2nd}{c}$$

d is the cavity length

n is the group refractive index

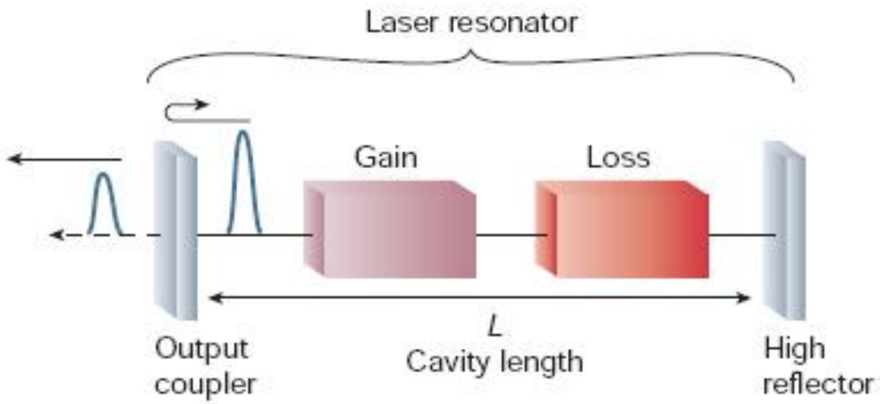

Cavity configuration in a passively mode-locked laser

$$E(t) = \sum_m A_m \exp j[(\omega_0 + m\delta\omega)t + \Phi_m]$$

$$E(t) = A_0 \left(\frac{\sin[(k+1)\delta\omega t_1/2]}{\sin[\delta\omega t_1/2]} \right) e^{i\omega_0 t}$$

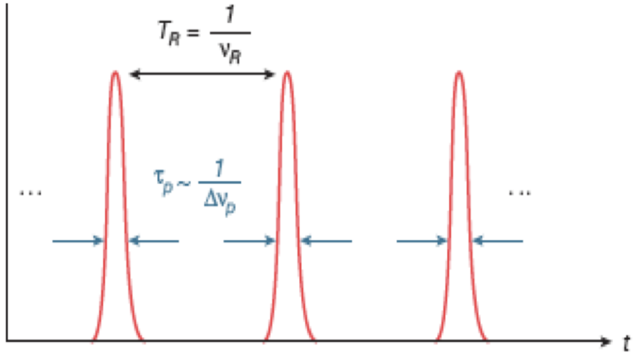

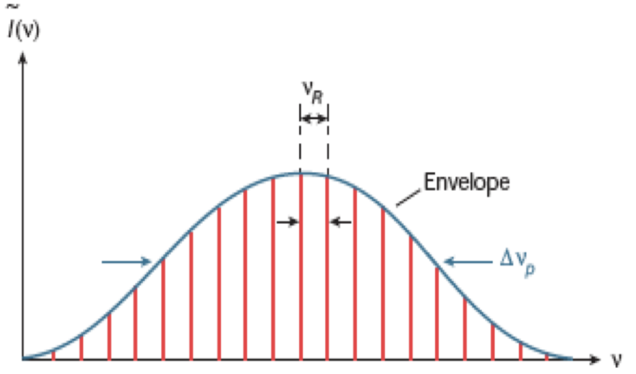

Mode Locking

❑ Active mode-locking

⇒ using an external signal to induce a modulation of the intra-cavity light;

⇒ the laser cavity contains an active element, such as an optical modulator

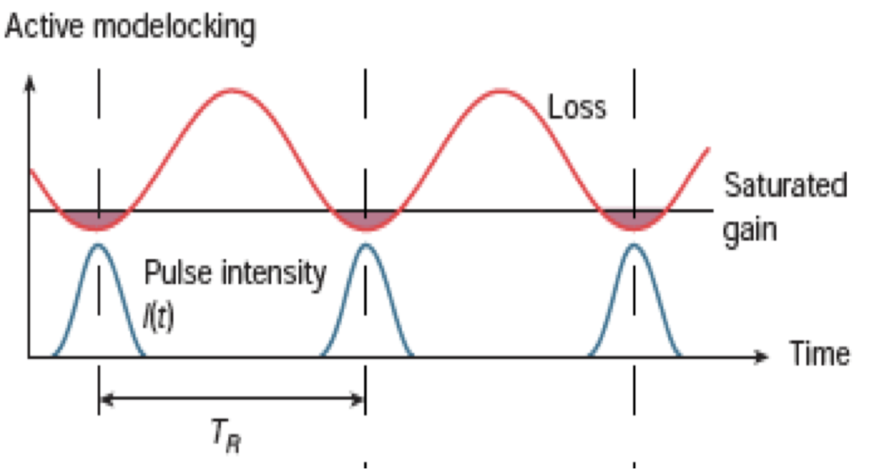

❑ Passive mode-locking

⇒ use a nonlinear passive element, such as a saturable absorber that leads to the formation of an ultrashort pulse circulating in the laser cavity and causes self-modulation of light

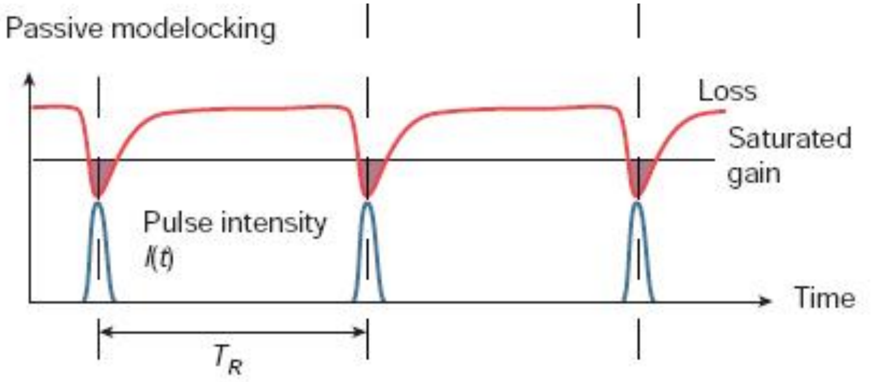

Pulse generation with a fast absorber in a passively mode-locked laser

CPML vs SCPML

- This method is based on the **interaction of two counter propagating optical pulses inside the absorber of a laser**

- If the **two pulses do collide in the absorber, they will effect a much higher degree of saturation of its loss than if the pulses were to arrive in sequence**

- Self-colliding pulse mode-locking

⇒ The location of absorber is next to a high reflection (HR)-coated mirror where **the optical pulse collides with itself in the saturable absorber for pulse narrowing**

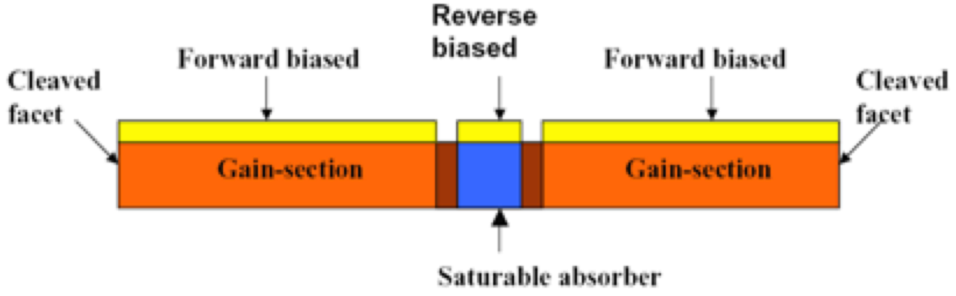

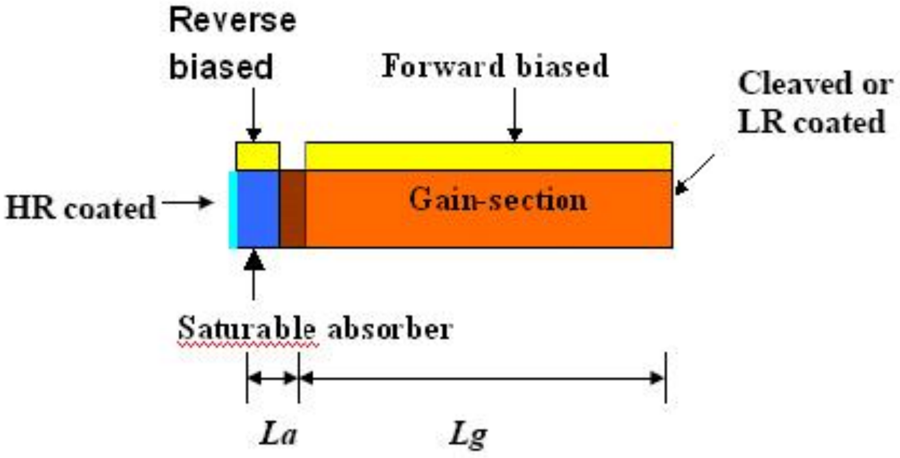

The configuration of a monolithic SCPM laser

QD for mode-locking

☐ Why Quantum dots are ideal source for mode-locking?

- ultrabroad bandwidth
- ultrafast gain dynamics
- easily saturated absorption
- strong inversion
- wide gain bandwidth

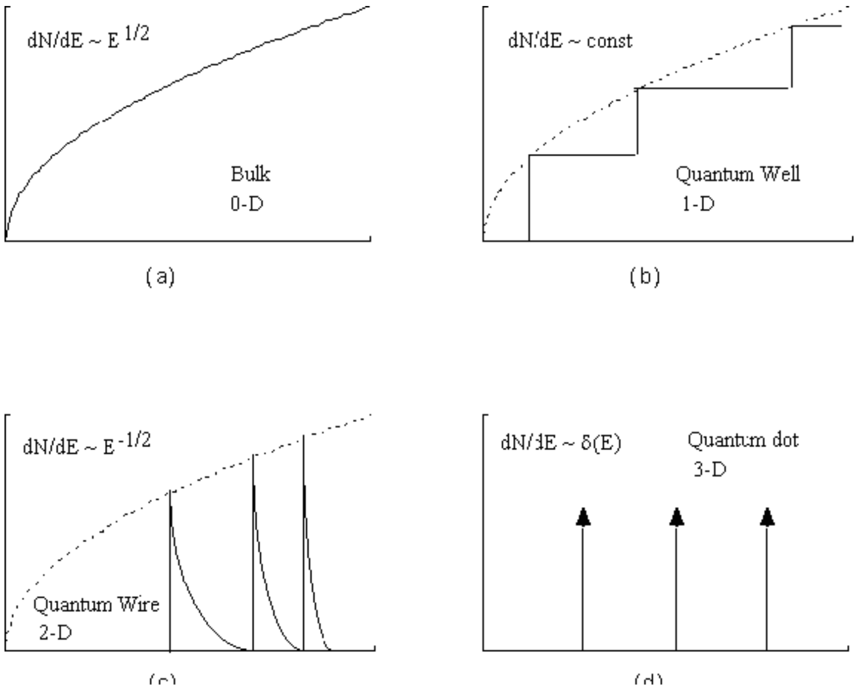

☐ Figure of merit for mode locking:

$$\frac{E_{sat,g}}{E_{sat,a}} = \frac{\frac{h\nu A_m}{\Gamma \frac{dg}{dN}}}{N_t h\nu A_m} = \frac{1}{\Gamma N_t \frac{dg}{dN}}$$

LCC

- Mode-locked lasers exhibit bi-stability in LCCs

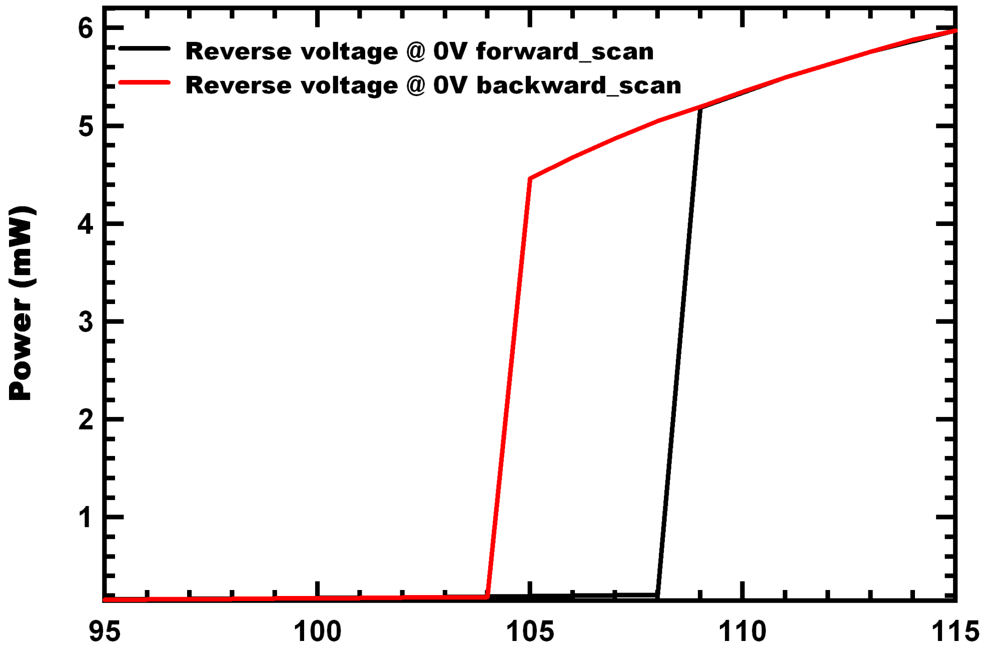

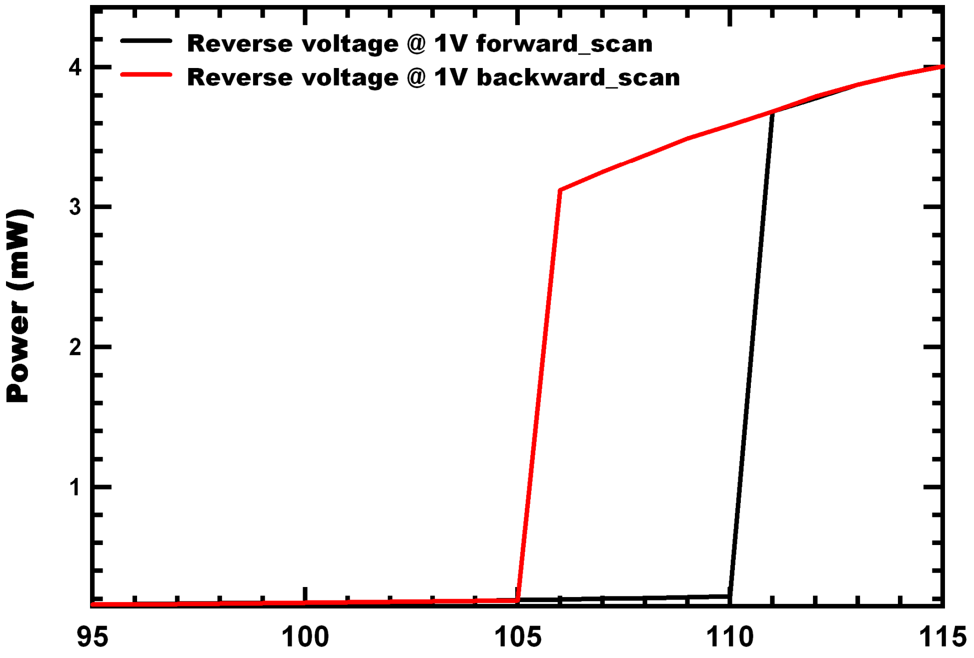

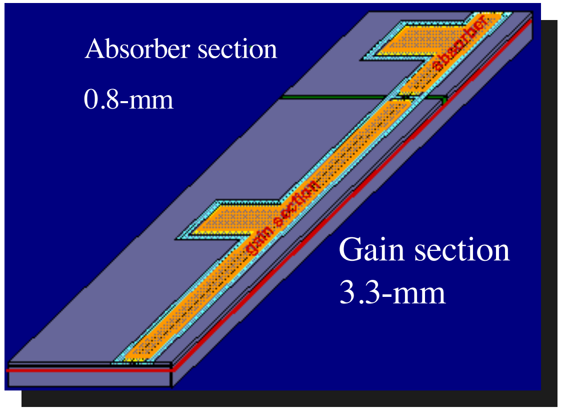

LCC curve with a reverse voltage of 0V on the 0.8-mm absorber

LCC curve with a reverse voltage of 1V on the 0.8-mm absorber

Electrical Spectrum

- ESA diagram:

a. 0V 200mA, full span

b. 0V, 200mA, span: 100MHz

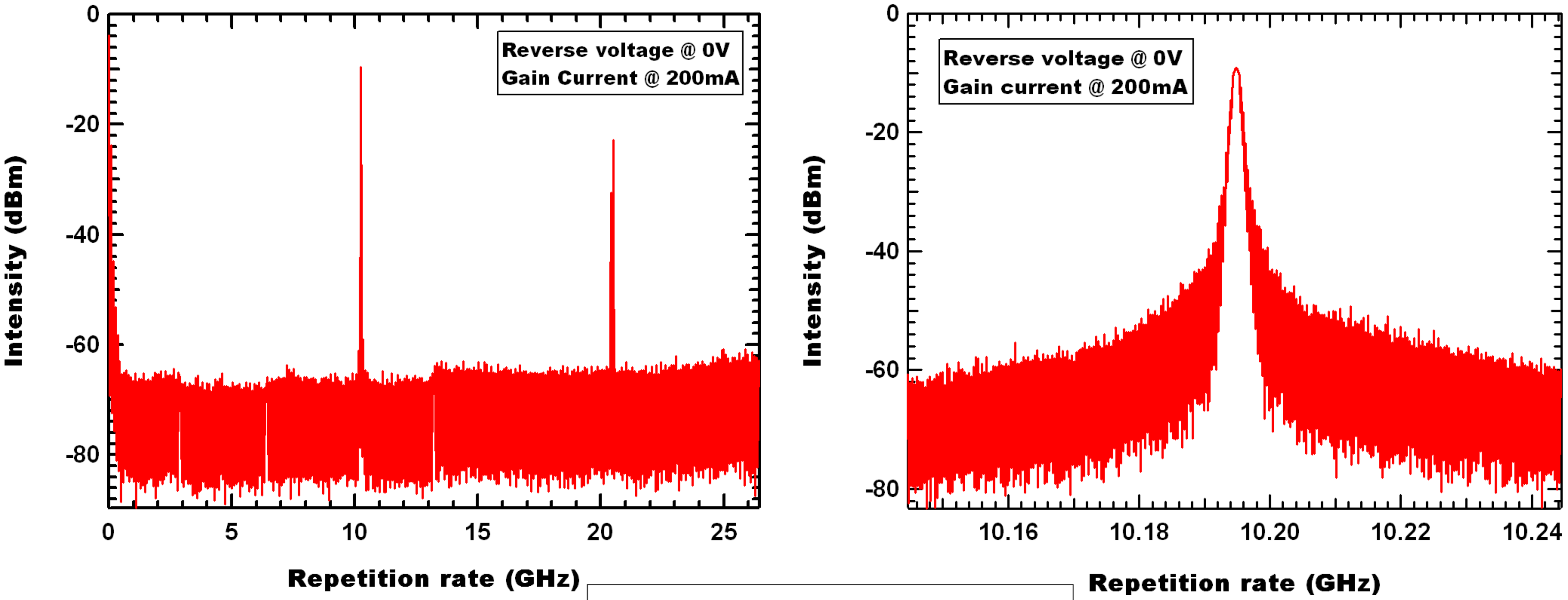

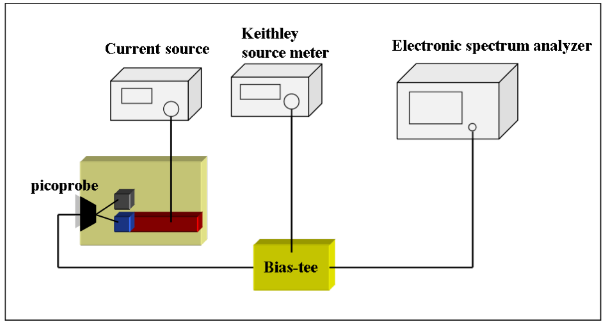

Electrical Spectrum

- ESA diagram:

  a -1V 200mA, full span

  b -1V, 200mA, span: 100MHz

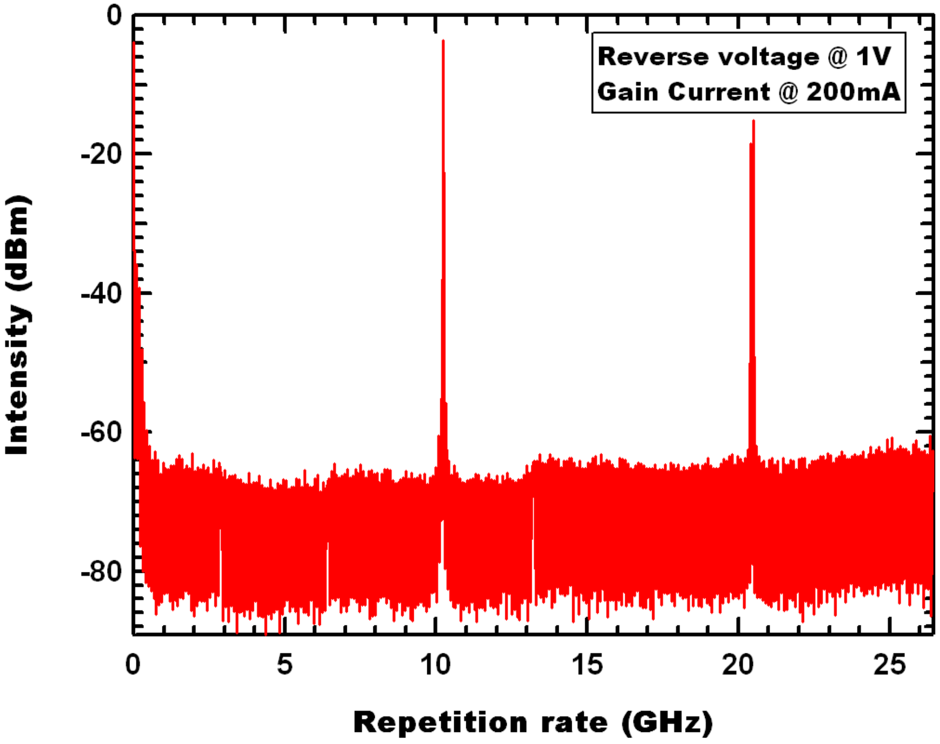

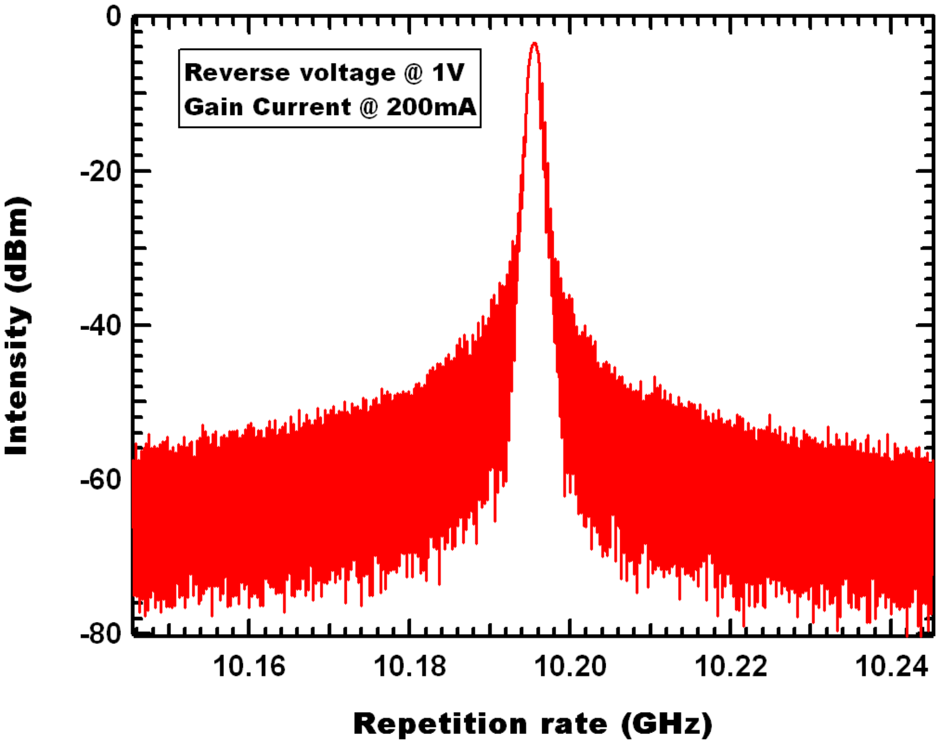

String Harmonics

- ❑ Creation of Node
  - Location of Node
- ❑ Artificial Harmonics
  - Simultaneous Placement of Nodes

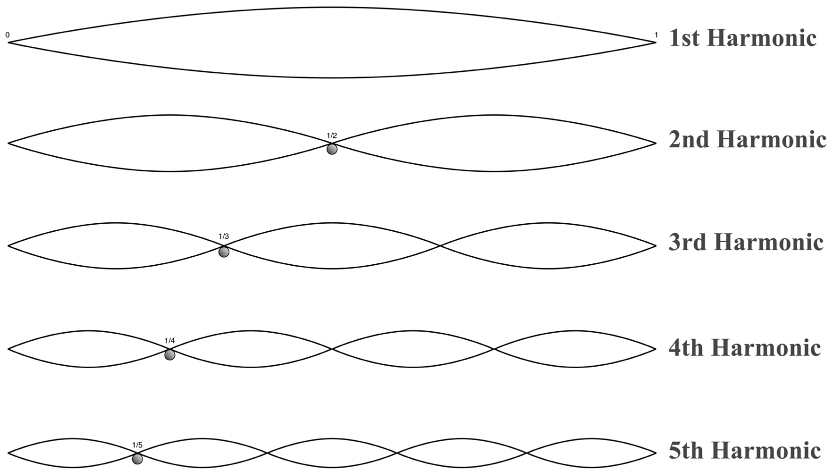

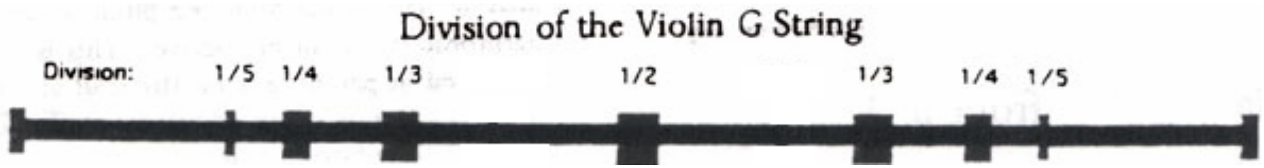

Location of Nodes on a Violin

Segmented Device

- Device
  - 6.75-mm
  - 3-µm Ridge
  - 27 Sections
    - 250-µm
  - HR~95%
  - AR~5%

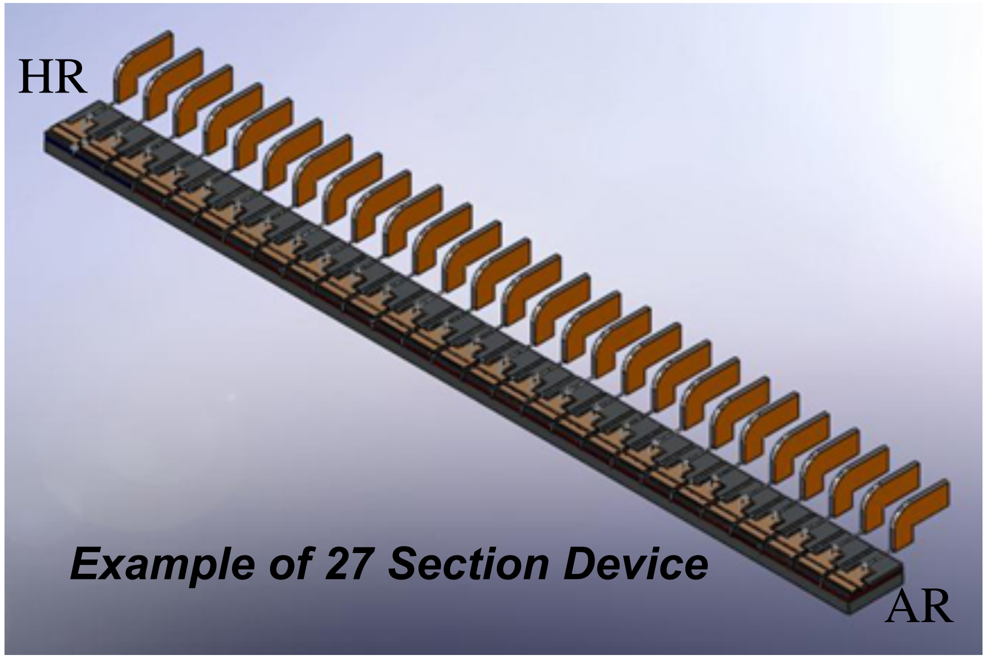

Example of 27 Section Device

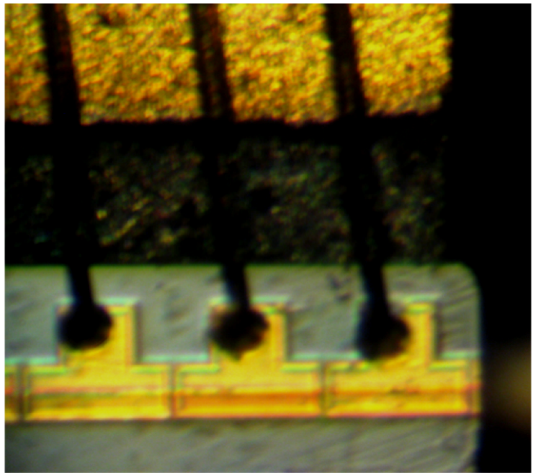

Image of the wirebonded device

Absorber Location

- ❑ Absorber Placement
  - *L* is Device Length

- ❑ Harmonic Stimulated
  - n^{th} Harmonic
  - *N is the n*umber of Equal Length Segments
  - *m* is the section number

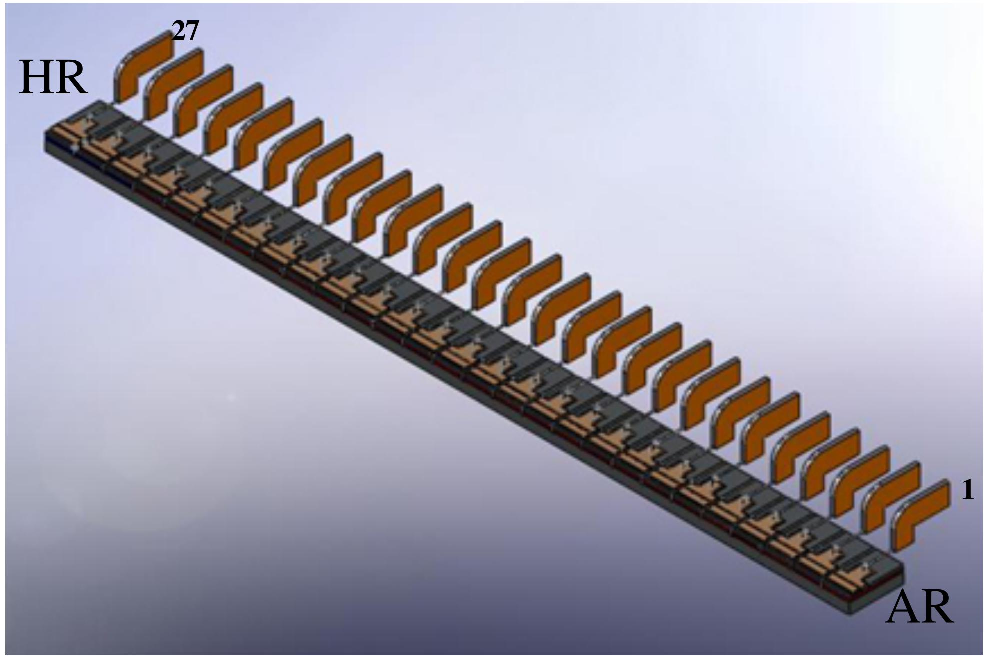

$$n = \frac{1}{\frac{1}{2} - \frac{1}{N} \cdot \left| m - \frac{(N+1)}{2} \right|}$$

Fundamental

- ☐ Sections 25-27
  - V_R= 3.15V
- ☐ Uniform Pumping
  - 150 mA
  - (555.56 A/cm^2)
- ☐ Pulse Width = 4.96 ps
- ☐ f_{Rep} = 6.019 GHz

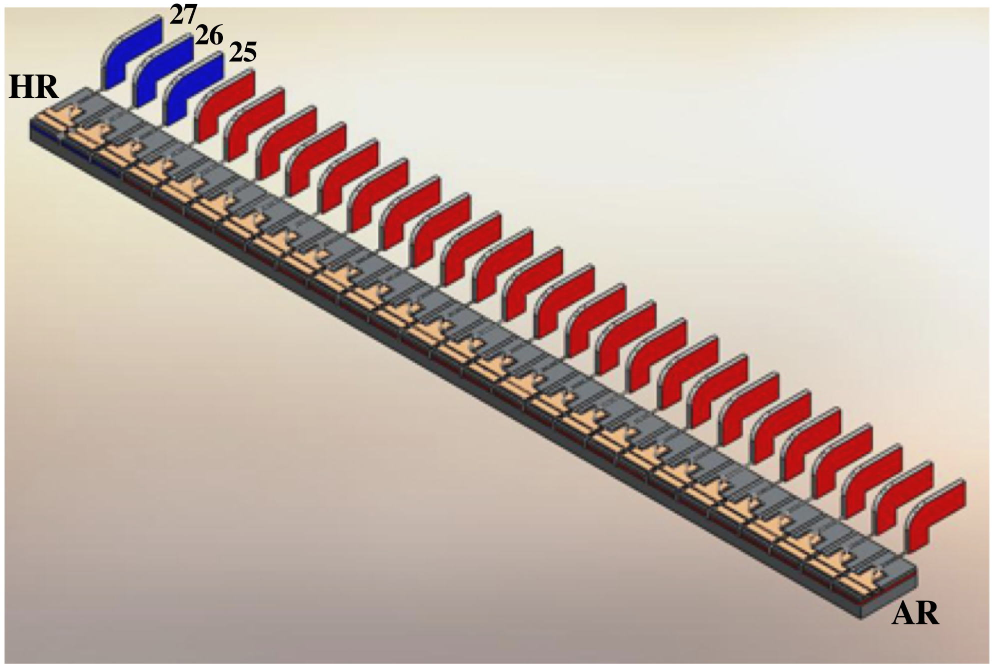

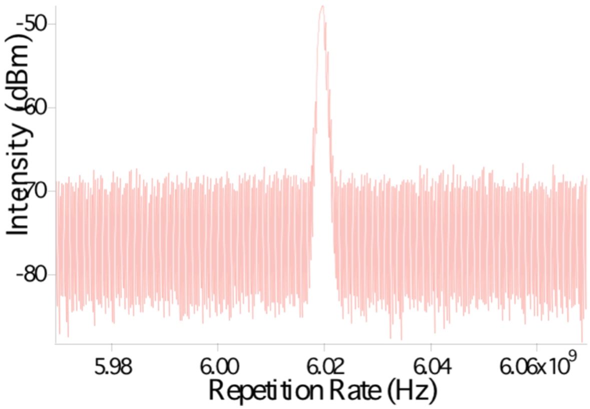

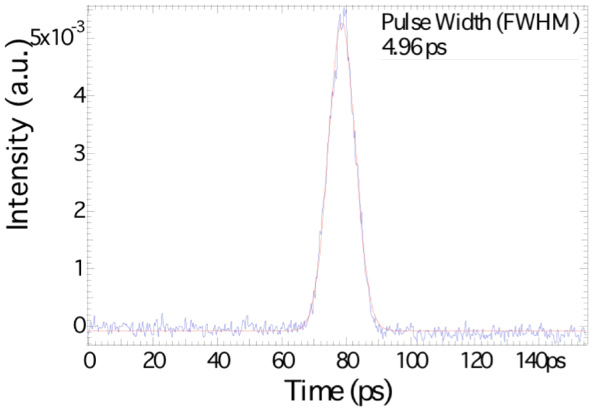

2nd Harmonic

- ☐ Section14
  - V_R= 4.49V
- ☐ Uniform Pumping
  - 150 mA
  - (555.56 A/cm^2)
- ☐ Pulse Width = 7.28 ps
- ☐ f_{Rep} = 12.027 GHz

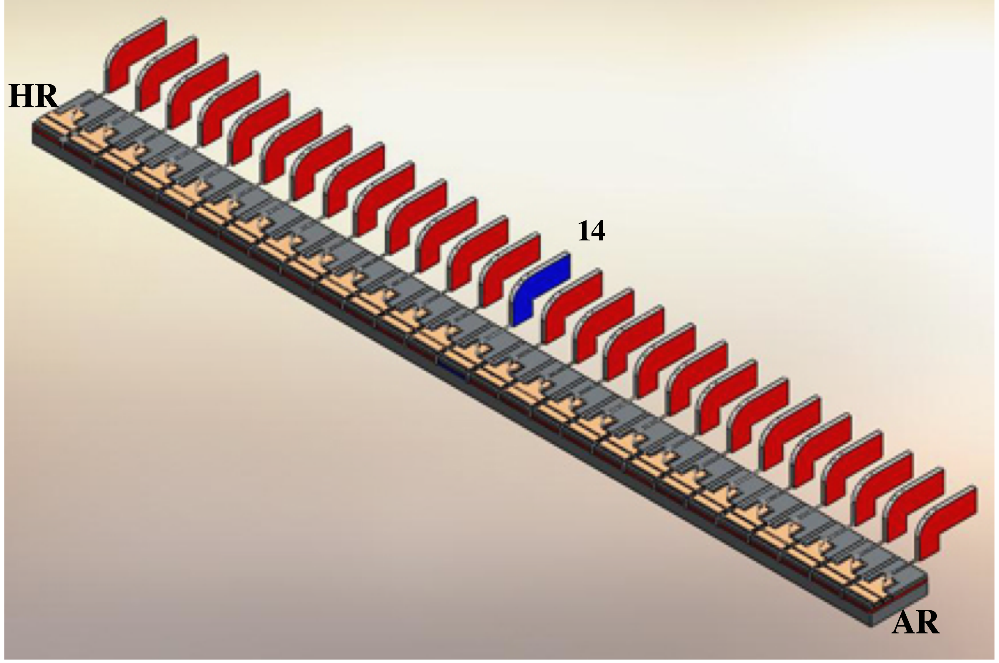

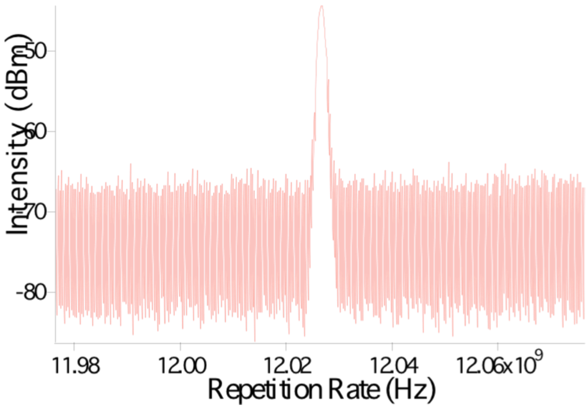

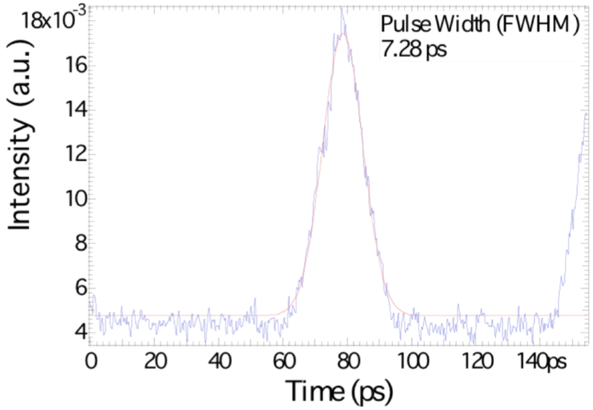

3rd Harmonic

- Sections 18 & 19
    - V_R= 3.38V
- Uniform Pumping
    - 150 mA
    - (555.56 A/cm^2)
- Pulse Width = 4.34 ps
- f_{Rep} = 18.023 GHz

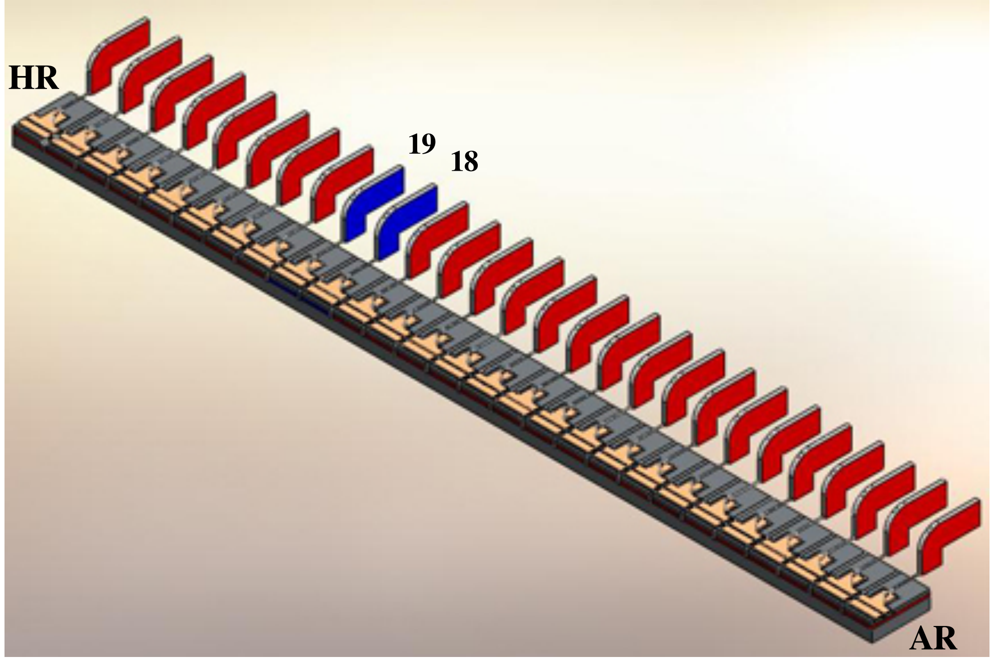

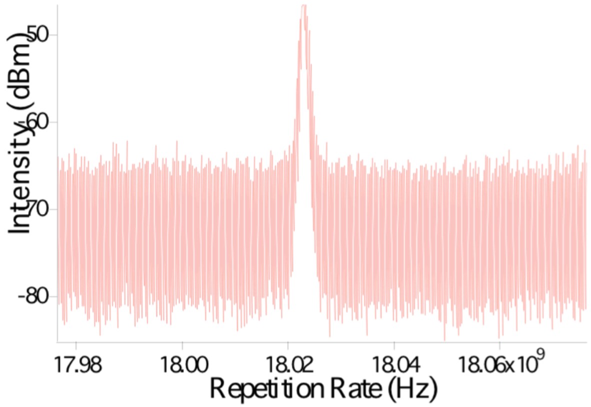

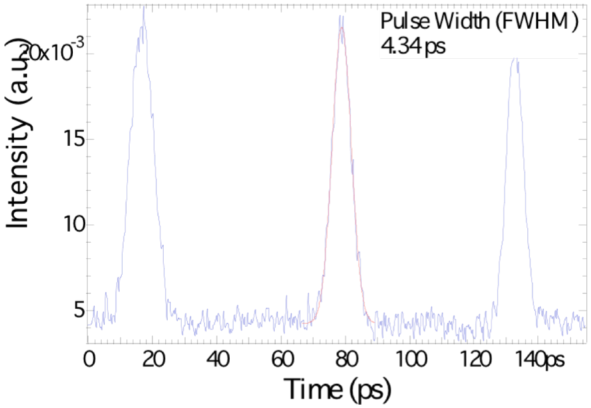

6th Harmonic

- Section 14
  - V_R= 2.14 V
- Sections 9 & 10
  - V_R= 0.00V
- Uniform Pumping
  - 300 mA
  - (1111.11 A/cm^2)
- Pulse Width = 6.82 ps
- f_{Rep} = 36.120 GHz